

DISSERTATION

CUSTOMER AND SYSTEM IMPACTS OF GRID SUPPORT FUNCTIONS FOR VOLTAGE
MANAGEMENT STRATEGIES

Submitted by

Julieta Giraldez Miner

Department of Systems Engineering

In partial fulfillment of the requirements

For the Degree of Doctor of Philosophy

Colorado State University

Fort Collins, Colorado

Summer 2020

Doctoral Committee:

Advisor: Siddharth Suryanarayanan

Rebecca Atadero

Liuqing Yang

Peter Young

Daniel Zimmerle

Copyright by Julieta Giraldez Miner 2020

All Rights Reserved

ABSTRACT

CUSTOMER AND SYSTEM IMPACTS OF GRID SUPPORT FUNCTIONS FOR VOLTAGE MANAGEMENT STRATEGIES

This document describes modeling techniques and methods to study the impacts to the utility and to the customer of using DERs such as advanced inverters to provide voltage support in order to maintain voltage within the recommended voltage limits. For this, a method for accurately representing secondary circuits in distribution feeders is proposed and quasi-static-time series (QSTS) simulation techniques are used to study the impact of advance inverter functions to the utility for managing voltage and to the customer in terms of possible generation curtailment. This dissertation looks at factors in medium and low-voltage circuit topology that drive customer voltages with DERs, and investigates where along the distribution feeder are voltage based advance inverter grid support function most effective. The described modeling techniques and methods have informed policy and regulatory type decisions such as updating DER interconnection tariffs and standards.

ACKNOWLEDGEMENTS

I would like to thank my advisor Dr. Siddharth Suryanarayanan for his guidance and perseverance in believing that I would complete this important achievement. I will also like to thank all of my NREL colleagues for their invaluable contributions, support and collaboration, specially Peter Gotseff, Andy Hoke, Michael Emmanuel, Michael Blonsky, Adarsh Nagarajan, Aadil Latiff, Killian McKenna and Nick Wunder. Also, a special thanks to Ben Kroposki from NREL for his mentorship and support. Finally, I would like to thank my parents Fernando and Cristina for inculcating in me the value of education, and for their unconditional love and support.

DEDICATION

I would like to dedicate this dissertation to my grandparents Moncho, Merche y Jose, and to my son Oscar.

TABLE OF CONTENTS

ABSTRACT	ii
ACKNOWLEDGEMENTS	iii
DEDICATION	iv
LIST OF TABLES	vii
LIST OF FIGURES	viii
Chapter 1	Introduction 1
1.1	Objective 2
1.2	Scope 3
1.3	Literature Review 3
1.3.1	Modeling and Simulation Techniques 4
1.3.2	DER Interconnection Standards 5
1.3.3	Advanced Inverters for Voltage Support 6
1.3.4	Modeling Techniques of Low-Voltage Secondary Distribution Circuits 8
1.4	Organization 9
1.5	Assumptions and Errors in Grid Models 10
Chapter 2	ch. 2 12
2.1	Introduction 12
2.2	Model Conversion and Steady-State Validation 13
2.3	Design of Secondary Circuits 15
2.4	Data processing for Time-Series Simulation 17
2.4.1	Replacing Missing and Outlier Data 18
2.4.2	Estimating Customer Loads 19
2.5	Time-Series Validation 21
2.6	Conclusions 23
Chapter 3	Effectiveness of DER Voltage-Based Grid Support Functions in Low-Voltage Secondary Circuits 26
3.1	Introduction 26
3.2	Low-Voltage Secondary Circuits and Characteristics from a Sample Subset 27
3.3	Comparison of Feeder Modeling Results with Representative versus Simplified Secondaries 33
3.4	Effectiveness of Real and Reactive Power from Customer-Sited DERs for Voltage Support 34
3.5	Modeling Low-Voltage Circuits for Hosting Capacity Studies 36
3.6	Conclusion 37
Chapter 4	ch. 4 38
4.1	Introduction 38
4.2	Voltage Based Grid Support Functions, Metrics and Impacts 40

4.2.1	Two voltage grid support functions	40
4.2.2	Volt-var in reactive and active power priority modes	42
4.2.3	Impacts of grid support functions	43
4.2.4	Metrics	44
4.3	Test Feeders, PV Penetration Cases and Grid Support Function Scenarios .	45
4.4	Results of High-Penetration PV Cases with Residential volt-var (VV) and volt-var-volt-watt (VV-VW) GSFs	47
4.4.1	Customer Energy Production Metrics	47
4.4.2	Customer Energy Curtailment versus Maximum Customer Voltage . . .	48
4.5	Conclusion	51
Chapter 5	ch. 5	52
5.1	Introduction	52
5.2	Autonomous Inverter-Based Volt-Watt Control	56
5.3	Methods for Estimating PV Energy Curtailment	56
5.3.1	AMI-Based Curtailment Estimation	56
5.3.2	Field Data-Based Curtailment Estimation	59
5.3.3	Simulation-Based Curtailment Estimation	60
5.3.4	Metrics for Assessing Proposed Method Accuracy	60
5.4	Evaluating Methods for Estimating Curtailment	62
5.4.1	Curtailment Estimation Based on AMI and Simulation Voltages	62
5.4.2	Curtailment Estimation Using Field Measurement	63
5.5	Performance Evaluation	66
5.5.1	Comparing results of the proposed AMI-based curtailment estimation with the VROS simulation	67
5.5.2	Comparing results of the proposed AMI-based curtailment estimation with the field measurement data	67
5.6	Conclusions	69
Chapter 6	Conclusions and Potential for Future Work	71
Bibliography	74
Appendix A	85

LIST OF TABLES

2.1	Impact of activating GSF control on PV systems and energy curtailment at different penetration levels	17
3.1	Energy Curtailed from Volt-Var and Reactive Power Absorbed by All Advanced Inverters	33
4.1	Scenario Description for M34 Feeder at various GDML PV Penetration Cases	47
4.2	Impact of activating GSF control on PV systems and energy curtailment at different penetration levels	48
5.1	Performance Metrics of the Proposed AMI-Based Methodology against the VROS simulation data	68
5.2	Comparing Field- and AMI-Based Curtailment Estimation for a Customer in Location A	68
5.3	Comparing Field- and AMI-Based Curtailment Estimation for a Customer in Location B	69

LIST OF FIGURES

2.1	Geographical view of L distribution feeder in the commercial distribution software on the left and OpenDSS on the right.	15
2.2	Percentage error of voltage (left) and sequence impedance (right) with respect to distance from the feeder head for feeder L.	16
2.3	Diagram showing the load and solar model provided by the utility on the left, and the detailed load transformer and secondary circuit added to the existing model for every load node.	18
2.4	Flowchart showing the methodology to assign a secondary design process to OH and UG residential customers from a total of 55 detailed secondary designs provided by the utility.	19
2.5	MWh/MW values versus irradiance for a fleet of PV systems in the M34 region. Note that the AM and PM values are in red and blue colors, respectively.	21
2.6	The L feeder gross real power from the MWh/MW method and PV system profiles.	22
2.7	Power (top) and voltage (bottom) time-series comparison between Grid 2020 distributed measurements and OpenDSS model at M3 transformer 1400 for September 16-17, 2016.	23
2.8	Envelope of maximum and minimum voltage across the secondary circuit of a service transformer location in which maximum and minimum simulated (top) and measured (bottom) voltage envelopes.	24
2.9	Voltage to distance from the substation plot of primary voltages (solid lines) and secondary voltages (dotted lines) for feeder L on May 23 at 12:30 p.m.	25
3.1	Customer electrical impedance for 10 overhead secondary designs.	28
3.2	Customer electrical impedance for 33 underground secondary designs.	29
3.3	Customer degree impedance for 10 overhead secondary designs.	31
3.4	Customer degree impedance for 33 underground secondary designs.	32
3.5	Timeseries Voltages for all Customers in Feeder M34 with no Advanced Inverters: a) Representative Secondaries (Left), and b) Star Secondaries (Right).	34
3.6	Timeseries Voltages for all Customers in Feeder M34 with Volt-Var: a) Representative Secondaries (Left), and b) Star Secondaries (Right).	34
3.7	Effectiveness of volt-var at reducing voltage rise across a secondary circuit.	35
4.1	The two voltage grid support functions and the settings used in this study	41
4.2	Volt-var reactive power and active power priority modes	43
4.3	Geographical view of M34 distribution feeder	46
4.4	Weekly customer energy curtailment versus maximum voltage for the low PV penetration case	49
4.5	Weekly customer energy curtailment versus maximum voltage for the medium PV penetration case	49
4.6	Weekly customer energy curtailment versus maximum voltage for the high PV penetration case	50

5.1	Hawaiian Electric’s approved volt-var and proposed volt-watt curves	57
5.2	Volt-watt curve showing maximum possible curtailed power	57
5.3	Conceptual illustration of estimated curtailment as a function of AMI voltage for a hypothetical day in which the voltage peaks at 1.1 p.u. (which is much higher than seen in field data and outside of tariff rules, but useful for illustrative purposes).	58
5.4	Proposed AMI-based method vs. VROS simulation curtailment estimates	63
5.5	A typical high voltage customer from the VROS simulation	63
5.6	Curtailment estimates for the typical high voltage customer from the VROS simulation	64
5.7	Field measurement at one of the selected advanced inverter locations	64
5.8	Field measurement-based curtailment estimates for a PV customer with volt-watt activation during a high-voltage period	65
5.9	Field measurement-based curtailment estimates for a PV customer with volt-watt activation during a normal voltage period	65
5.10	PV inverter power vs. AC voltage showing upper cutoff of the volt-watt curve and relationship to DC-bus voltage (dot color)	66
5.11	Probability density function for voltage data points during the high-voltage period . . .	67

Chapter 1

Introduction

From the beginning of the 2000s, the price of distributed energy resources (DERs) has decreased enough to make technologies such as distributed photovoltaics (PV) affordable to many segments of the market. The cost of crystalline modules decreased from \$4/W in 2006 to less than \$0.40/W in 2016. Lower costs are helping PV systems in many markets achieve grid parity, particularly in those with high retail rates [1]. Other small-scale generation and storage technologies have decreased in cost more recently as well [2]. In parallel, consumers are demanding increase in customer choice, particularly customers interested in contributing to a cleaner environment [3].

Safely integrating DERs into the utility grid is a critical aspect of the proliferation of customer-sited resources . The power grid was designed to transmit the power over long distances from power plants typically located far away from the energy consumers, and finally distribute the power to end users at lower voltages. For decades, the distribution system hosted a passive one-way power flow and utilities did not have much automation, data and situational awareness to safely plan and incorporate DERs in the grid. However, DERs such as distributed PV have changed the paradigm, and have accelerated the urge for utilities to modernize the grid and technology providers to make DER technology more “grid friendly”, to ultimately plan for the grid of the future in which energy customers are demanding more services than just being provided with affordable power.

From the distribution utility perspective, the major grid impact of DERs such as residential and commercial distributed PV is consistent high voltages, that push customer voltages outside the recommended voltage tolerance region specified in the ANSI C84.1 standard [4]. When a customer exports power during the day, when their consumption is low and their irradiance is high, there can be local voltage rise. Traditional utility voltage regulation equipment located on the primary or medium voltage sections of feeders, such as substation transformer Load Tap Changer (LTC), line voltage regulators and capacitors, can be adjusted to accommodate this voltage rise. However, the primary sited legacy voltage regulation equipment is not very effective at mitigating the high

voltage conditions that occur on the feeder secondaries or low voltage circuits. Leveraging new technology such as advanced inverters in PV or storage systems, as well as controlling load, can help mitigate the high voltage impacts locally where the voltage rise occurs. The implementation of DERs providing voltage support can be performed in an autonomous fashion, in which DERs or load, respond to local voltage measurements, or in a centralized way in which DERs and loads receive control settings from the utility or an entity providing the voltage support service. Presently, the focus of the architecture from the utility and regulatory side in the US has been to first activate local grid support functions such as voltage and frequency support functions, and then enable the communication, software and infrastructure requirements to implement future centralized control strategies. Utilities see investments in future systems that can integrate advanced inverters into distribution grid operations as foundational to full realization of DER potential [5]. Advanced Distribution Management Systems (ADMS) and Distributed Energy Resource Management Systems (DERMS) software will provide visibility and control of advanced DER functionalities to the utility and allow DERs to fully realize their value through dynamic management for distribution grid services. Protocols for communicating to DERs are being developed, such as the SunSpec Common Smart Inverter Profile in California [6] and more broadly the IEEE 2030.5 [7]. However, there is not yet a solution that allows seamless interoperability between DERs and utilities.

1.1 Objective

The focus of this dissertation is on modeling techniques and methods to study the impacts to the utility and to the customer of using DERs such as advanced inverters to provide voltage support in order to maintain voltage within the recommended voltage limits. To study this question in a modeling and simulation environment, individual customer voltages need to be accurately represented in order to closely approximate the local voltage measured at the customer meter, since this is the point to which DERs autonomously react to. Accurate simulation of low voltage circuits also enables to understand in more detail where along the secondary the grid support functions are

effective at providing voltage support. This modeling techniques and methods can inform policy and regulatory type decisions such as updating DER interconnection tariffs or standards.

1.2 Scope

The scope of this work is to investigate a method for accurately representing secondary circuits in distribution feeders and to use quasi-static-time series (QSTS) simulation techniques to study the impact of advance inverter functions to the utility for managing voltage and to the customer in terms of possible generation curtailment. This dissertation looks at factors in medium and low-voltage circuit topology that drive customer voltages with DERs, and investigates where along the distribution feeder are voltage based advance inverter grid support function most effective.

This work evaluates fixed voltage grid support function settings, versus studying the optimal grid support function setting, and evaluates the activation of the same setting for all customer-sited DERs. Also, this work does not consider communication enabled DER control architecture in which DER voltage grid support function settings can change depending on the optimal strategy to be implemented and rather focuses on local or autonomous DER controls based on local grid conditions.

Finally, this work studies the distribution system for steady-state voltage management strategies at time-steps greater than minutes, and thus does not address any concerns related to voltage stability control problems that can arise at a faster timescale. The voltage control functions evaluated are implemented with internal inverter control loops in the "seconds" time-scale, and as such, there are no expected adverse interactions when deploying volt-var and volt-watt advanced inverter controls [8].

1.3 Literature Review

In this section a review of the modeling and simulation techniques to evaluate the impacts of customer-sited resources in the distribution system is provided, followed by a description of the important standards driving the interconnection of such resources with the power grid. Next,

the advanced inverter concept and studies evaluating their capacity to provide services to the grid are presented, and finally a review of the less-explored topic of modeling techniques for the low-voltage edge portion of distribution feeders is included.

1.3.1 Modeling and Simulation Techniques

For decades, utilities relied on steady-state power flow analyses of distribution feeders based on critical time periods such as peak and minimum loading points to evaluate the impacts on the distribution system. Such steady-state power flow studies, also commonly referred to as snapshot analysis, would only give the magnitude of an impact at one instant in time, which was sufficient when load was the sole driver of the distribution system for design and operation. For example, in a passive distribution network, the voltage management strategy for a feeder is designed and evaluated at peak and minimum loading conditions with load tap changer transformers, step voltage regulators and switched capacitors sized and operated to maintain customer voltages within acceptable limits [9]. However, with the proliferation of customer-sited resources, such as PV, injecting power into the distribution system transforming the network into a two-way power flow system, there are more variables influencing the design and operation of the system such as the variable and uncertain behaviour of renewable energy resources. One or a few snapshots of power flow evaluations of the distribution system may not appropriately capture the effects of time-dependent resources on the distribution system. A draft of the IEEE P1547.7/D11 guide on conducting DER distribution impact studies for distributed resource interconnection discusses four types of special system impact studies: (1) dynamic simulation, (2) electromagnetic transient (EMT) simulation, (3) harmonic and flicker study, and (4) quasi-static simulation [10]. QSTS solves a series of sequential steady-state power flow solutions where the converged state of each iteration is used as the beginning state of the next. This captures time-varying parameters such as load and the time-dependent states in the system such as regulator tap positions. QSTS simulation is best defined by the IEEE P1547.7/D11 draft guide: “*Quasi-static simulation refers to a sequence of steady state power flow, conducted at a time step of no less than 1 second but that can use a time step of up*

to one hour. Discrete controls, such as capacitor switch controllers, transformer tap changers, automatic switches, and relays, may change their state from one step to the next. However, there is no numerical integration of differential equations between time steps.” [10]

The notion of time-series power flow simulations is discussed in the literature for impact studies of different DER: solar PV [11–14], wind [15, 16], electrical vehicles [17, 18], and energy storage [19–21]. The principal advantage of QSTS simulation is that it attempts to properly capture time-dependent aspects of power-flow influenced by multiple drivers, e.g., weather, customer behaviour and rate structures. In [22], the authors describe a guide and study procedure to perform high penetration PV analysis, including the importance of the data types and data-resolution. QSTS simulation, when compared to steady-state, requires time-series data to feed the simulation, as well as to validate the time-series model, and such time series data is often difficult to obtain [23]. In [24], the authors discuss the importance of the time resolution in the data driving the discrete simulations in order to be able to draw solid conclusions, for instance with regards to voltage regulation equipment operations.

1.3.2 DER Interconnection Standards

Technical standards and codes are important to define the rules and procedures to safely interconnect customer-sited technologies into a utility power system. In this subsection we focus on the standards that apply the point of common coupling (PCC), i.e. the grid interconnection point between a customer and a utility.

The family of standards that apply to the PCC between a customer DER and the utility are the Institute of Electrical and Electronics Engineers (IEEE) 1547 interconnection standards. These include IEEE 1547-2003: IEEE Standard for Interconnecting Distributed Resources with Electric Power Systems, which was the first important effort to regulate the requirements for DER interconnection. The philosophy in this early series of standards was to not have DERs actively regulate voltage or frequency so that they would not interact with the legacy utility operational voltage and frequency management strategies as well as to have DERs trip when a fault is detected

in the system. In April 2018, a major revision to IEEE 1547 was published, IEEE-2018 Standard for Interconnection and Interoperability of Distributed Energy Resources with Associated Electric Power Systems Interfaces [25]. This prescribes that DERs shall be capable of: 1) actively regulating voltage, 2) riding through abnormal voltage/frequency, 3) providing frequency response, and, finally, 4) may provide inertial response. This revision has been critical to standardize not only how DERs are interconnected at the PCC with the utility system but also how they should interact and actively participate in the safe operation of an electric grid. The standard also references the point of interconnection, which might have different applications than the PCC for some DER systems. This revision enables DERs to actively regulate voltage and frequency to help manage a grid and thus contribute to the safe operation of a power system that has higher penetration levels of renewable energy resources when required by regulators and a utility.

Some regions that are already experiencing high penetrations of distributed PV have taken their own initiatives to set specific regional requirements for the interconnection of DERs. For example, in California there is Rule 21, Hawai'i has Rule 14H, Europe has the recently approved European Wide Technical Specifications (FprTS 50549-1/2 and EN 50438:2013), and Australia has the AS 4777 standard. For further reading on global PV interconnection standards, please refer to [26].

1.3.3 Advanced Inverters for Voltage Support

Developing power electronics made it possible for PV inverters to have advanced functionalities such as reactive power support, ride-through capability, and real time communications with operators [27]. Recently, having PV inverters to participate in maintaining stable and reliable operations is being considered as a solution to integrate additional PVs onto the grid [28]. In the future smart grid architecture, it is likely that many PV systems will be connected to a communications network, allowing an advanced centralized or distributed control system to coordinate the inverter. But currently, many PV systems are not connected to any communications network. The inverters that are connected communicate typically solely with the proprietary server of a vendor, but not with the utility, and only when the internet connection of the customer is active. Therefore,

the most feasible way for PV inverters to support the grid is by autonomously responding to local conditions (i.e., to the voltage waveform the inverter measures at its terminals) in a way that stabilizes voltage and frequency. In this section we provide a review of advanced inverters for voltage support.

NREL and San Diego Gas and Electric (SDG&E) looked at modeling of volt-var and fixed power factor, however, load and PV systems were represented at the aggregate level at the primary of the service transformers [29]. The study also considered oversized inverters, watt priority, and volt-var support during non-PV-producing hours. The study concluded that smart PV inverters installed in sufficient quantity at the right location can impact a distribution circuit voltage by providing reactive power support with the inverter operating at fixed power factor settings or in volt-var mode. Lastly, SolarCity and NREL looked at the estimated impact of PV systems with volt-var control on voltage-reduction energy savings and distribution system power quality on two utility feeders (one Hawaiian Electric and one Pacific General Electric), and concluded that voltage-reduction energy savings increased with volt-var control, and that they also had a positive impact on the power quality [30]. This work included a star network approximation for the Hawaiian Electric feeder for secondary low-voltage circuits, i.e. one generic secondary model with service a transformer and a dedicated service line for each customer from the transformer. Reference [31] investigated the impacts of various penetration levels of advanced inverters on a typical distribution network showing that smart inverters have the capability to improve tap operations, voltage variability, and minimum and maximum voltages. Reference [32] presented a methodology for the optimal settings of a group of advanced inverters using autonomous inverter control and revealed that optimal settings depend on inverter kVA rating, feeder layout, load and solar characteristics.

While the effectiveness of grid support functions is apparent, it can cause energy curtailment to PV customers. For instance, advanced inverter controls allow PV inverter systems to support reactive power priority by curtailing active power output when required to keep the grid within its operational constraints [33–35]. The authors in [33] argue that there is no obvious nexus between

increased reactive power output and decreased PV kWh generated and show that the application of volt-var control could mitigate voltage violations without causing PV active power curtailment. A method to design a smart inverter volt-watt control to mitigate possible voltage violation for a high PV penetration case while curtailing energy evenly among all integrated PV systems is presented in [36]. In [37], techniques to create distribution models for determining the effectiveness and impacts of various GSFs were presented. This topic is further expanded in the following subsection 1.3.4.

1.3.4 Modeling Techniques of Low-Voltage Secondary Distribution Circuits

As previously introduced, it is becoming critical to improve the modeling and simulation of customer voltages to understand the integration of grid-edge control techniques that leverage the grid-friendly capabilities of customer-sited resource such as advanced inverters in PV systems and other DERs.

Utility companies in the United States have put considerable effort toward improving the way they represent distribution systems, and have sizeable portions of their distribution feeders represented in a commercial distribution software tool such as Synergi Electric, CYME, or DEW. To the best knowledge of the author these models lack accurate or realistic representations or models of the low-voltage secondary networks. In [38], the authors discuss North American split-phase secondary circuits in detail and compare the full 120-V split-phase models with the single-phase equivalent at 240 V. They find that the load unbalance fully represented in full split-phase models has only a minor influence on the accuracy of the simulated 240-V load voltages and that single-phase equivalent model can be used to accurately represent split-phase secondary circuit 240-V voltages but should not be used to represent unbalanced 120-V load voltages. In [39–42], the authors propose a series of measurements driven methodologies to estimate and validate low-voltage secondary circuits based on AMI and PV system data in case study on the Georgia Tech campus. Reference [43] describes a statistical analysis based on a clustering technique to come up with representative low-voltage networks out of a large (over 200) sample of designs in the North West

of England. This work applies well to 50Hz systems, but not to 60Hz systems. In this thesis, a method to assign secondary low-voltage circuits to primary nodes based on sampled secondaries is proposed for two distribution feeders in Oahu, Hawai'i [34, 37]. This methodology is then used in [44] for six PGE feeders. These studies in Hawai'i and California are the only known references that include a more sophisticated method to approximate customer voltages in the US.

1.4 Organization

This dissertation is organized as follows. Chapter 2 provides an overview of the low-voltage modeling technique proposed in this dissertation for distribution feeder modeling for QSTS of voltage management strategies [34, 37]. This research was used in public hearings and official regulatory dockets to justify the activation of voltage grid support functions in Hawai'i and California, which resulted in new requirements for DERs to provide voltage support as stipulated in the in the state level interconnection standards¹. Chapter 3 provides an overview of sampled characteristics of low-voltage circuits that drive voltage rise with customer sited DERs, and investigates the effect of both reactive and active power based voltage grid support functions on voltage support along a distribution systems. Chapter 4 presents the results of evaluating voltage grid support function impacts to the utility and the customer [35, 45]. Chapter 5 concludes and provides directions for future work.

The main contributions of this work can be summarized in two main areas: 1) modeling techniques to quantify customer impacts of advanced inverters, and 2) the application of the research results. The key scientific contributions in the modeling area are firstly, the development of a method to assign a pool of secondary low-voltage circuit designs to customers in a feeder, and secondly, the development of a method to estimate customer curtailment from the activation of advanced inverter functions. The key scientific contribution in the application of the methods here proposed are that this work raised for the first time the issue of the importance of more accurately

¹Rule 14H in Hawai'i was updated in November 2017 to require volt-var, and CA Rule 21 was update in December 2017 to require volt-var and volt-watt.

modeling the grid-edge of distribution circuits, as well as quantifying the impacts to residential customers of the activation of advanced inverter functions.

1.5 Assumptions and Errors in Grid Models

The methods and results presented in this dissertation are based on building complex distribution system models that attempt to represent as accurately as possible the present operating condition of the distribution grid, over which future scenarios can be built to answer distribution planning questions. However, modeling based results carry the inherent problem of how accurate the models are, and how confident researchers are with the results they produce given the number of assumptions that go into simplifying the real world in a simulation environment. Here, the assumptions and possible sources of errors in the models proposed are described, as well as why the results can be used with confidence by the research, industry and broader stakeholder community.

Sources of errors in the distribution models that are proposed in this dissertation are:

- Error in utility feeder model built from a GIS database of grid infrastructure
- Error in the conversion of the utility feeder model to the open source software OpenDSS
- Error in approximating customer load and generation profiles
- Error in the approximation of the grid-edge infrastructure that is not in the original utility feeder model

Given the above mentioned sources of uncertainty with grid modeling and simulation techniques, it is critical to be able to check with field measurements that the results produced by complex models align with what is being measured in the field. As such, it was critical to build confidence in the simulation results produced by the research presented in this dissertation, to have field measurements, as presented in Chapters 2 and 5. In addition to the field measurements used to calibrate and compare the model results, EPRI also applied some of the methods proposed in this research in another utility service territory, and obtained very similar results as the ones here produced [44].

At last, it is always important to understand the order of magnitude of accuracy that models are trying to predict. In this case, the goal of the distribution grid model was not to recommend day-to-day operational and control strategies for which a higher level of accuracy in predicting voltages may be required. In the contrary, this research attempts to answer distribution planning questions, as well as to inform policy makers, such as public utility commissions, of the order of magnitude of the impact of "set and forget" autonomous settings for PV systems.

Chapter 2

Distribution Feeder Modeling for QSTS of Voltage Management Strategies²

2.1 Introduction

Utilities and technology developers are increasingly interested in understanding the impacts of distributed technology and customer-sited resources on distribution feeder operations. To simulate how distributed technology such volt-var devices or photovoltaic (PV) inverters with grid support functions (GSF) integrates into legacy utility voltage management schemes, it is very important to create models of the utility distribution system that accurately represent the present field operations. This paper describes some techniques to prepare and validate real utility distribution feeder models for quasi-static time-series (QSTS) power flow simulation. The baseline QSTS models can then be modified to create scenarios that can be compared to current utility operations.

It is increasingly important to represent as accurately as possible the voltage ranges that are measured at customer locations because utilities are modifying existing distributed energy resources (DER) interconnection standards to enable DERs to regulate voltage. The present U.S. interconnection standard, IEEE 1547-2003 [46], prohibits DERs from actively regulating voltage. Exceptions to the standard can be made with the agreement of the utility and the PV owner, but such exceptions are rare. However, the ballot draft revision to IEEE 1547 will also require DERs to be capable of the GSFs [47]. In recognition of the fact that DER-based voltage support is needed at higher penetration levels, both California and Hawai'i have published interconnection rules requiring various GSFs starting in September 2017. In response to these changes, Underwriters Laboratories (UL) published UL 1741 Supplement SA (UL 1741 SA) procedures to validate inverter behavior for volt-var, volt-watt, and constant power factor among other grid support func-

²This chapter is published in [37] and the copyright is included in Appendix A

tions. To better understand how customer-sited resources will impact utility operations, creating good baseline models of the current utility operations to compare with future scenarios is an important step in research studies. Previous studies that looked at customer-sited resources with GSFs created time-series models of real utility feeders [14, 29, 48]. However, the load and PV systems in those models were represented at the aggregate level at the primary of the service transformers, or secondary circuit approximation was a star network design, which is often far from the field design.

This paper presents techniques to create baseline models using a utility feeder from Hawaiian Electric Company. These techniques were used in [34, 35, 45] to determine the effectiveness of various GSFs at regulating voltage and quantifying annual energy curtailment to solar PV customers. The rest of this paper is organized as follows: Section II describes the software-to-software conversion and steady-state validation of a utility feeder model; Section III describes a methodology to add secondary low-voltage circuit models to the utility feeder model; Section IV presents data processing techniques to create time-series data of customer load and PV profiles; Section V presents the time-series validation of the model; and, Section VI concludes.

2.2 Model Conversion and Steady-State Validation

Recently, utility companies across the U.S. made considerable effort toward improving the way they represent distribution systems, and have sizeable portions of their distribution feeders represented in commercial software environments. However, these environments have a paying license fee, and do not have DERs, particularly inverter based PV-powered, modeled to the level of detail necessary to conduct research studies. For this reason, the GIS-based feeder model from the distribution modeling software that the Hawaiian Electric Companies use is converted to the open-source distribution modeling software, Open Distribution System Simulator (OpenDSS) that is used in this paper for simulation voltage regulation operating strategies with PV inverters providing GSF. To validate this software-to-software conversion, the steady-state (one time-step) power flow solutions with planning loads from the commercial software environment and OpenDSS are

compared. This paper does not commercialize the OpenDSS software nor does it support its exclusive use for such studies; rather, the authors present it as one of the freely available software options for conducting such distribution studies. The example utility distribution feeder in this study, denoted “feeder L”, is converted from the commercial distribution software to OpenDSS. This conversion uses an automated Python[®] script developed at the National Renewable Energy Laboratory (NREL) that uses network configuration (.xml) and line configuration (.txt) as inputs. To use the tool, the feeder model provided by Hawaiian Electric in Microsoft Access database format was opened in the commercial distribution software and then exported in Extensible Markup Language (XML) format. Additionally, the line impedance information also was extracted from the commercial distribution software and used as an input by the tool. The conversion tool takes the two files described (i.e., the feeder in .xml format and the line construction report in .txt format) as inputs and creates a folder with the OpenDSS files. Then, the user can open the master circuit file and run it in OpenDSS.

The steady-state verification of the OpenDSS model was performed based on the following metrics: 1) the similarity in feeder topology between the converted model to the original model (based on visual inspection); and, 2) the difference between the node voltages and sequence impedance values for the converted model and the original model (less than 5%). The steady-state validation is performed by solving a power flow with the given planning load from the commercial distribution software calculated via load allocation from supervisory control and data acquisition (SCADA) data measured at the substation.

Figure 2.1 shows the topology of the feeders from the commercial distribution software and the converted model in OpenDSS. From Figure 2.1 it can be observed that the line distances and coordinates are appropriately converted. The subsequent step for verification compares the voltages and sequence impedances obtained from OpenDSS with those obtained from the commercial distribution software. Figure 2.2 (left) presents the voltage comparison, along with the errors, and Figure 2.2 (right) presents the sequence impedance and comparison errors for feeder L. The maximum error in voltage comparisons between the commercial distribution software and OpenDSS is

0.5% for feeder L. The maximum error in sequence impedance comparison between the commercial distribution software and OpenDSS is 2%. Although the maximum error is 2%, relatively few occurrences of errors are greater than 1%, as shown in the histograms in Figure 2.2 (right).

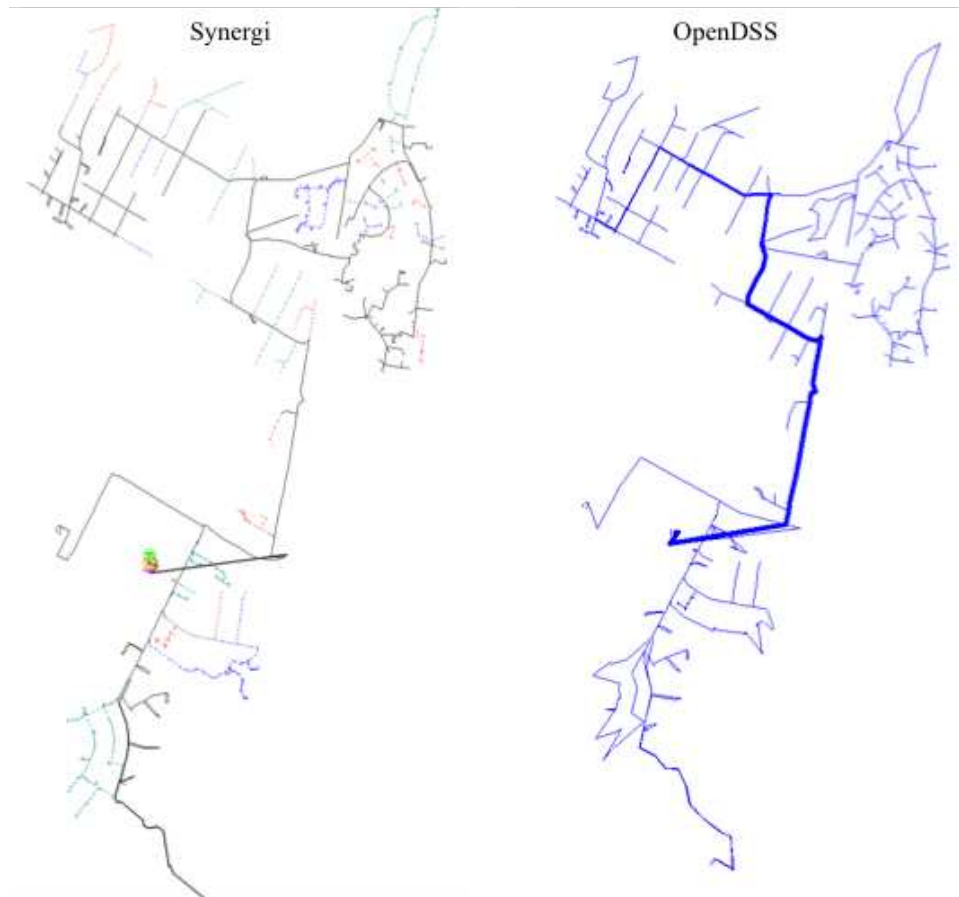


Figure 2.1: Geographical view of L distribution feeder in the commercial distribution software on the left and OpenDSS on the right.

2.3 Design of Secondary Circuits

Recently, utility companies represent distribution feeders in commercially available distribution software tools to conduct planning studies. To the best knowledge of the authors, however, there is no utility that has accurate or realistic representations or models of the low-voltage secondary networks. It is critical to add this level of detail to more accurately capture not only the

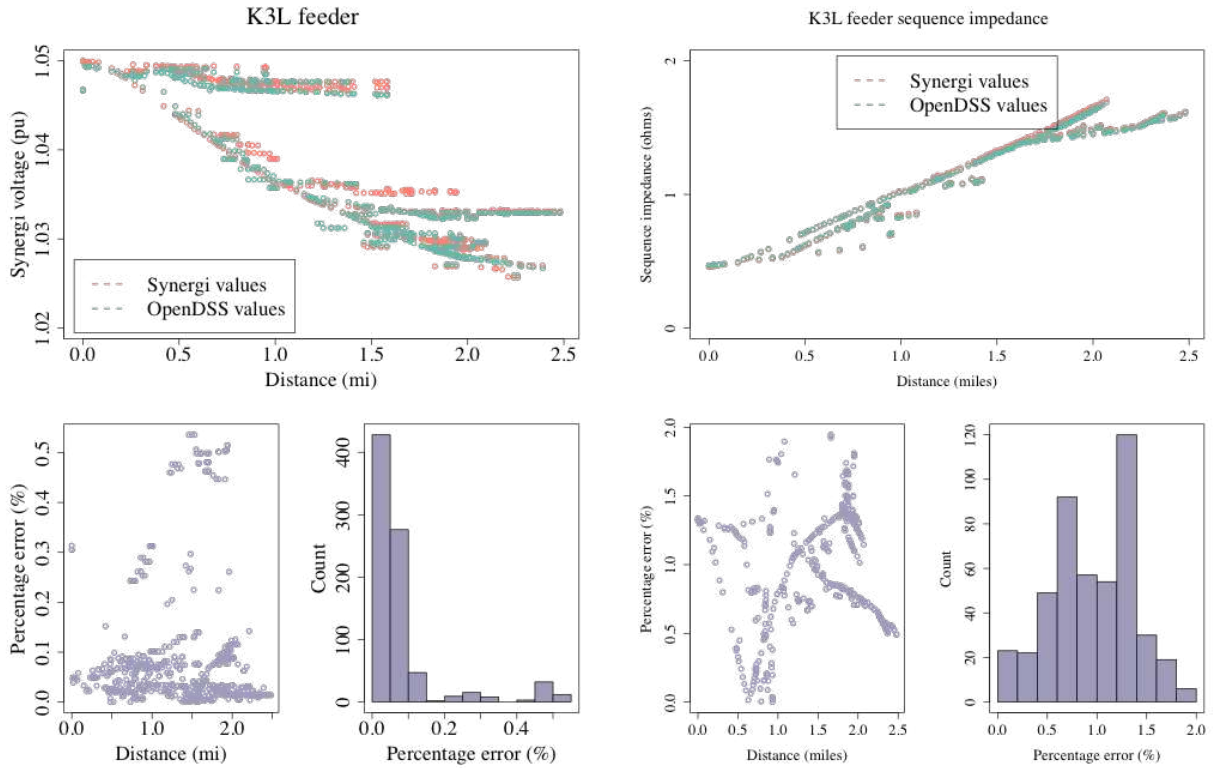


Figure 2.2: Percentage error of voltage (left) and sequence impedance (right) with respect to distance from the feeder head for feeder L.

annual voltages at the primary medium-voltage level, but also at the secondary low-voltage level to which PV systems are connected and required to meet tariff requirements.

To add accurate representations of secondary circuits, the aggregate load nodes (or service transformer nodes) in feeder L are classified into customer types to design secondary circuits based on this customer classification. This is followed by automating the building of such circuits in OpenDSS. The goal is to add more detail to the medium-voltage distribution models, including service transformers and secondary circuits in the OpenDSS model as shown in Figure 2.3, to capture the voltage drop that occurs from the medium-voltage bus to the customer residence, where the PV system inverters are connected. Ultimately, accurate simulations of the voltage at the terminals of the residential inverters are desired. Most of the advance inverter modes are control functions that depend on the local voltage sensed by the inverter, and thus emphasize the importance of capturing the voltage drops in secondary circuits. To classify load nodes into customer types, the

Table 2.1: Impact of activating GSF control on PV systems and energy curtailment at different penetration levels

Customer Type	Description of Secondary Designs (x Number of Designs)
M3 UG Residential	Housing developer detailed drawings (x 30)
M4 UG Residential	Housing developer detailed drawings (x 11)
Feeder L UG Residential	HECO secondary upgrade designs (x 3)
OH Residential	HECO secondary upgrade designs (x 11)
OH Rural	NREL proposed design

coordinates of each load node were superimposed on the land-use type. The GIS department at NREL performed this task. The customer types are selected based on the GIS classification and the availability of secondary designs. Hawaiian Electric provided 55 detailed designs for adding low-voltage circuits to the existing model. The Hawaiian Electric team was consulted to determine that the commercial and multifamily aggregated load nodes will be kept at the primary level in the model, because there is no significant voltage drop expected at those customer locations with typically oversized secondary circuits by design in order to accommodate larger real and reactive power draws. For the overhead rural customers, the following secondary build-out assumptions were considered: (1) customers are 200 ft. apart from each other; (2) overhead #2 cable size is used for secondary lines; and, (3) there are six customers per shared secondary circuit. This is followed by building the secondary circuits for underground (UG) and overhead (OH) residential customer types according to the flowchart diagram in Figure 2.4. The methodology is based on matching the service transformer size and the number of customers per transformer to the pool of secondaries described in 3.1 and the real values from the field. The process is automated in Python[®] to create the OpenDSS files of all secondary service transformers, lines, and each load representing a house and existing customer PV systems.

2.4 Data processing for Time-Series Simulation

A critical step in this effort is the synthesis of the data that will derive the time-series model. The data obtained from the utility for this process is: 1) substation SCADA voltage, current, and real and reactive powers for 2015; 2) individual feeder SCADA voltage, current, and real and

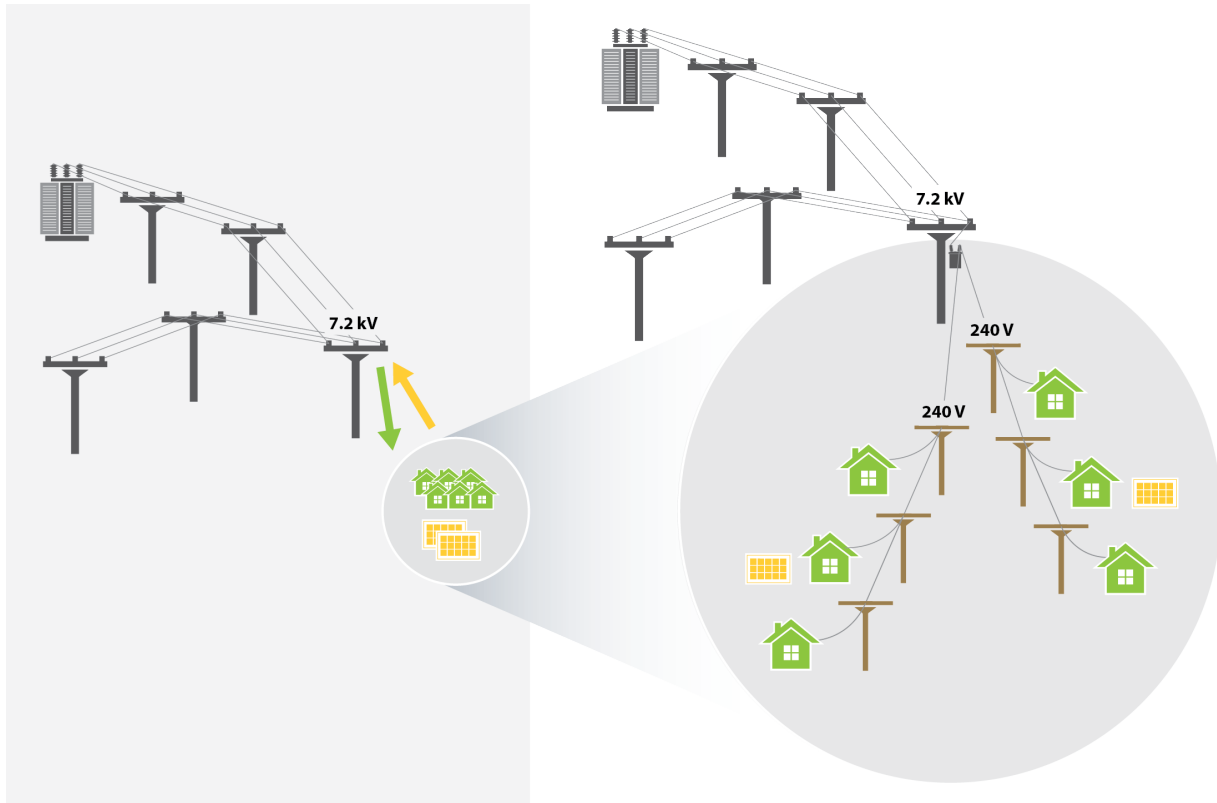


Figure 2.3: Diagram showing the load and solar model provided by the utility on the left, and the detailed load transformer and secondary circuit added to the existing model for every load node.

reactive powers as available for 2015; 3) megawatt-hours/megawatt PV power production for two PV regions of interest on Oahu, 4) 15-minute irradiance profiles for the two PV regions of interest on Oahu, and 5) 15-minute data on kilowatt-hour and voltage from the customer meter through Advanced Metering Infrastructure (AMI).

2.4.1 Replacing Missing and Outlier Data

The first step in the data-processing task is to identify missing and outlier data and replace it. An example of outlier data is a reconfiguration event in which a feeder picked up loads from a circuit in another substation, which is shown by abnormally high loading. Due to the good correlation of circuits within a substation, circuit data due to load transfer events were replaced with the adjacent circuit data connected to the same substation. For missing data (when there were

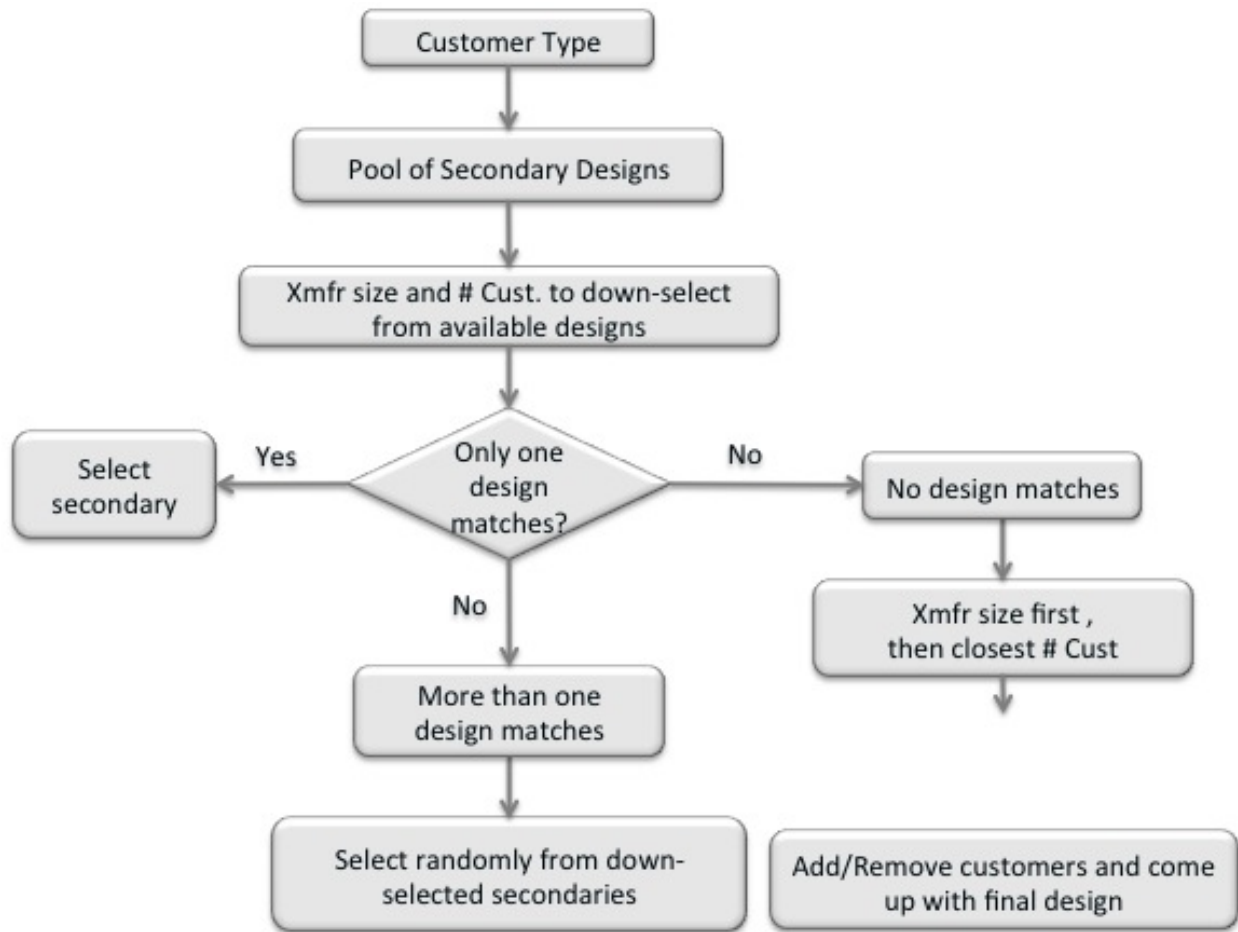


Figure 2.4: Flowchart showing the methodology to assign a secondary design process to OH and UG residential customers from a total of 55 detailed secondary designs provided by the utility.

overall SCADA outages) the data was replaced with the most appropriate adjacent (in time and day of week) time series data.

2.4.2 Estimating Customer Loads

The following section describes the estimation of the gross load (also sometimes referred to as "native" load), i.e. the load profile if there was no PV system installed in the feeders. During nighttime hours, the gross load and the measured SCADA data net load are the same. During daytime hours, however, the objective is to determine the shape of the demand without PV production. This gross-load profile can be used for estimating unknown load profiles among customers. Two methods are explored for this purpose: 1) real to reactive power regression method (PQ regression); and,

2) MWh/MW method. The real to reactive power linear regression at night is used to determine the real power during daytime hours. This PQ regression method only works for circuits that serve residential customers predominantly with invariable power factor during nighttime hours. This assumption also works only if the existing solar PV systems are connected at unity power factor. The advantages of using the PQ regression method are that it relies on power measurements, and it is independent of estimating how much PV energy is in the system and its profile. The other method explored for estimating gross load is to estimate the PV production for each of the feeders and subtract that from the SCADA net load at each time step. For this, the utility provided MWh/MW values versus irradiance of a fleet of systems in the feeder L region. The MWh/MW values account for the orientation and losses of PV systems. Figure 2.5 shows the AM and PM values highlighted in red and blue, respectively. The degree 3 polynomial fit of the distribution of all of the values is described in (2.1).

$$y = 3.293e^{-10}x^3 - 7.418e^{-7}x^2 + 1.243e^{-3}x^2 \quad (2.1)$$

where y is the energy per MW and x is the plane of array (POA) irradiance. The polynomial MWh/MW curve multiplied by the total installed PV systems rating (MW) for each circuit gives an estimate of the PV production at every given time step. Note that the MWh/MW curve was provided at an hourly resolution, and the SCADA net load is processed at 15-minute time steps. Because the utility also provided typical 15-minute POA irradiance curve for the geographical region of interest, an estimated final MWh/MW 15-minute curve using the irradiance profile is found. The PQ regression method could not be used on feeder L due to the presence of large inductive loads during daytime hours, making the PQ regression method invalid because it is based on nighttime real and reactive power correlation. Thus, feeder L circuit required the use of the MWh/MW method. Feeder L had approximately 1 MW of peak load (corresponding to 85 aggregate load nodes in the distribution model) that is not metered through AMI for which the substation load profile shown in Figure 2.6 using the MWh/MW method was used. For the time-series simulation, the available AMI customer data was used to derive the load profiles of individual customers. For

the customers that are not in the AMI program, the substation load multiplier as shown in Figure 2.6 is used to derive the non-AMI loads.

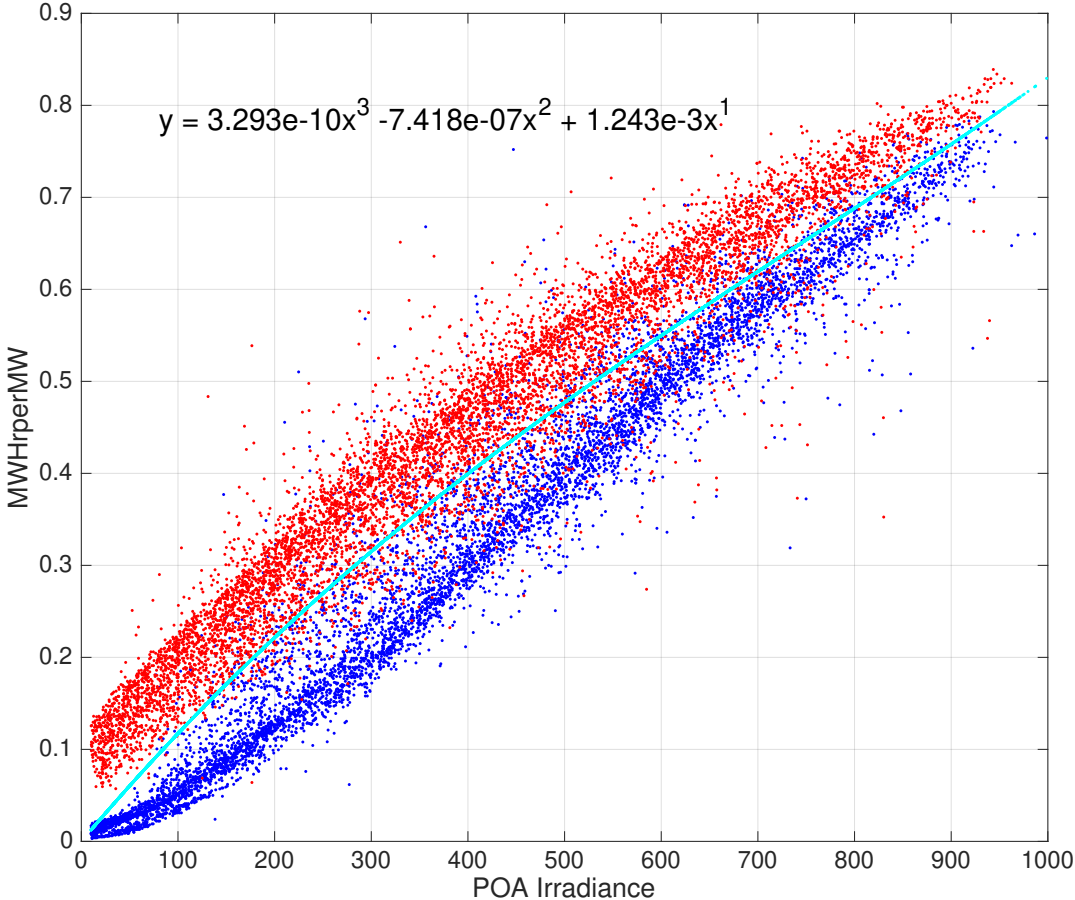


Figure 2.5: MWh/MW values versus irradiance for a fleet of PV systems in the M34 region. Note that the AM and PM values are in red and blue colors, respectively.

2.5 Time-Series Validation

The results of deriving the OpenDSS time-series model with the multipliers are shown in Figure 2.7 at the secondary of a service transformer. These are compared to the real power and voltage data measurements provided by the utility. When comparing voltages at the measurement location, the voltage profile of the OpenDSS model follows a similar timeseries profile when compared to

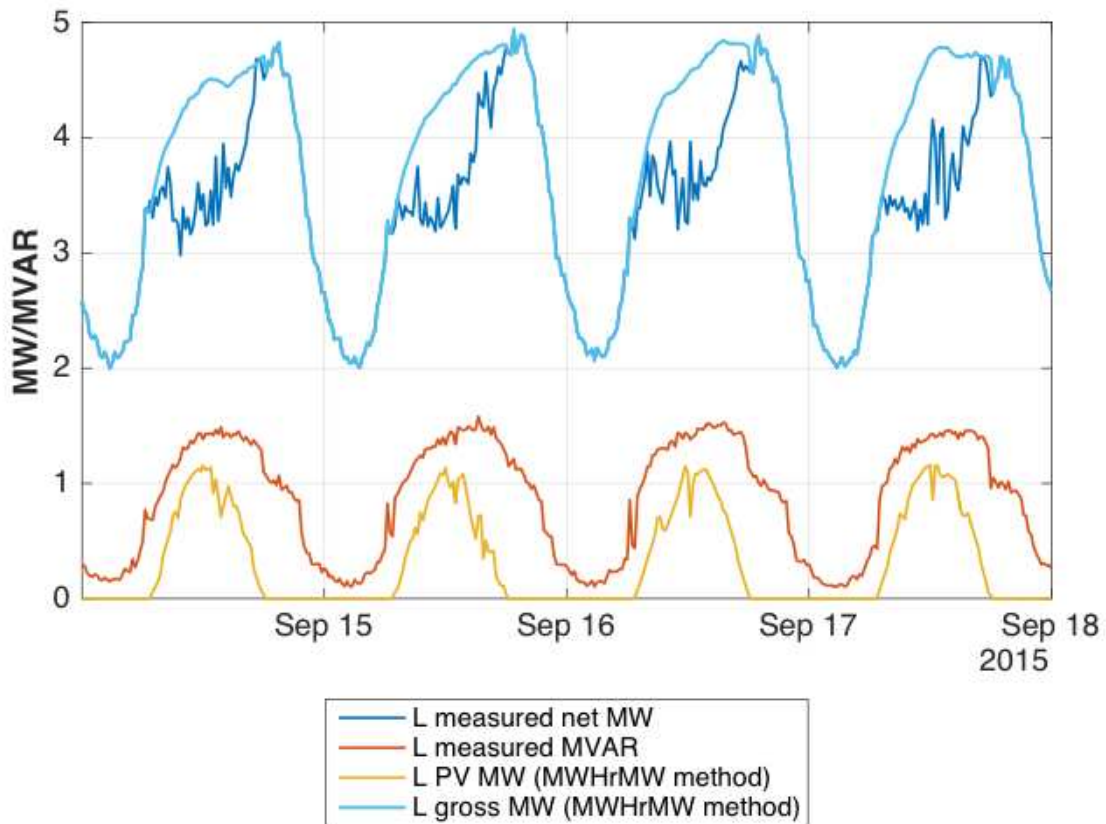


Figure 2.6: The L feeder gross real power from the MWh/MW method and PV system profiles.

the field data. Note that the legacy LTC in the model is behaving akin to its field performance, as observed by the step changes and voltage profiles driven by the LTC regulation in both field and modeled voltages. Figure 2.8 shows the voltage envelope comparison plots between the simulated and measured AMI voltage data for a service transformer location. The exact representation of secondary distribution circuits in the model and exact locations of the AMI meters were not available; rather, only which service transformer the AMI meters are connected to was known. So, the comparison is of the envelope (maximum and minimum) of the simulated and the measured customer voltage data connected to the same transformer. The maximum and minimum demonstrate how well estimated the voltage is at the beginning and at the end, respectively, of a secondary circuit.

Figure 2.9 shows the voltage to distance from the substation plot for feeder L; primary voltages are relatively flat, and the bulk of the voltage drop or rise occurs in the service transformer

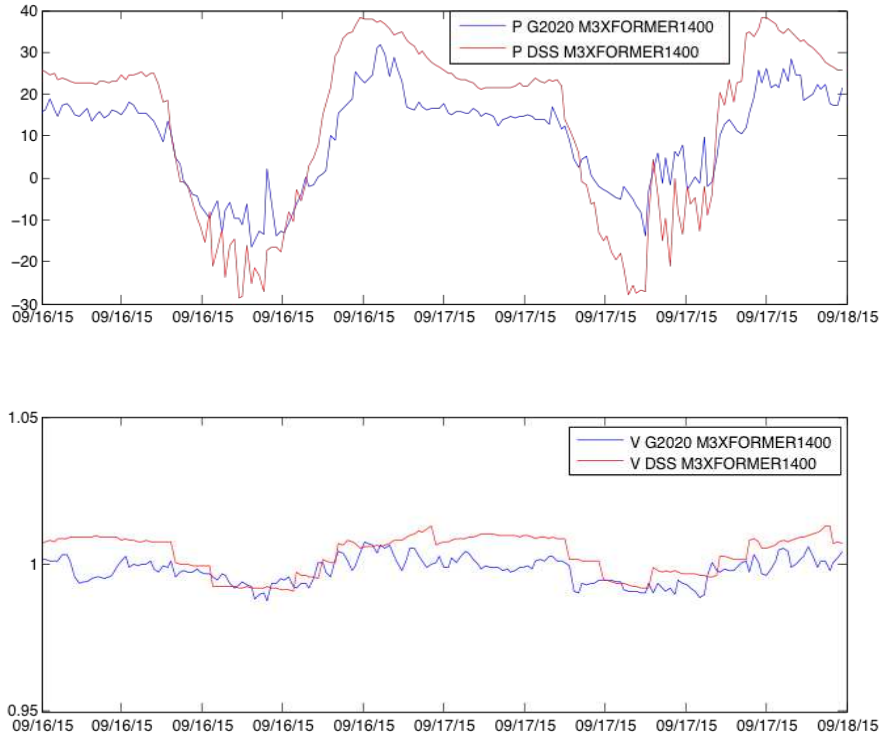


Figure 2.7: Power (top) and voltage (bottom) time-series comparison between Grid 2020 distributed measurements and OpenDSS model at M3 transformer 1400 for September 16-17, 2016.

and secondary circuits. This demonstrates the importance of the effort to approximate secondary circuits as accurately as possible to capture the local voltage that will be used for voltage based control functions at customer-sited resources such as advanced PV inverters.

2.6 Conclusions

This paper presents techniques to create baseline models using a utility feeder from Hawaiian Electric Company. It describes a software-to-software conversion and steady-state validation results of a utility feeder model and presents a methodology to add secondary low-voltage circuit models to the utility feeder model. The utility circuit is then validated with time-series measurements and the results show the importance of approximating secondary low-voltage circuits to accurately capture voltage at the customer meter level. Creating and validating baseline models of the current utility operations is important to compare with future scenarios in which customer sited resources are integrated in the operation of distribution systems.

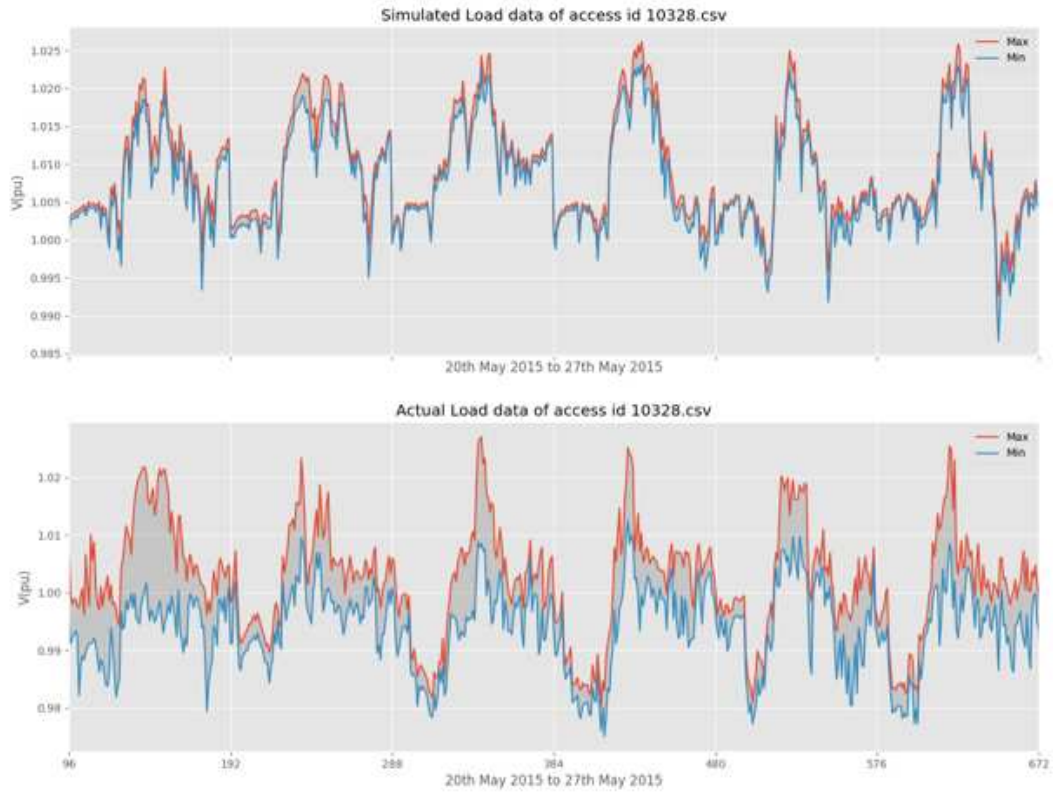


Figure 2.8: Envelope of maximum and minimum voltage across the secondary circuit of a service transformer location in which maximum and minimum simulated (top) and measured (bottom) voltage envelopes.

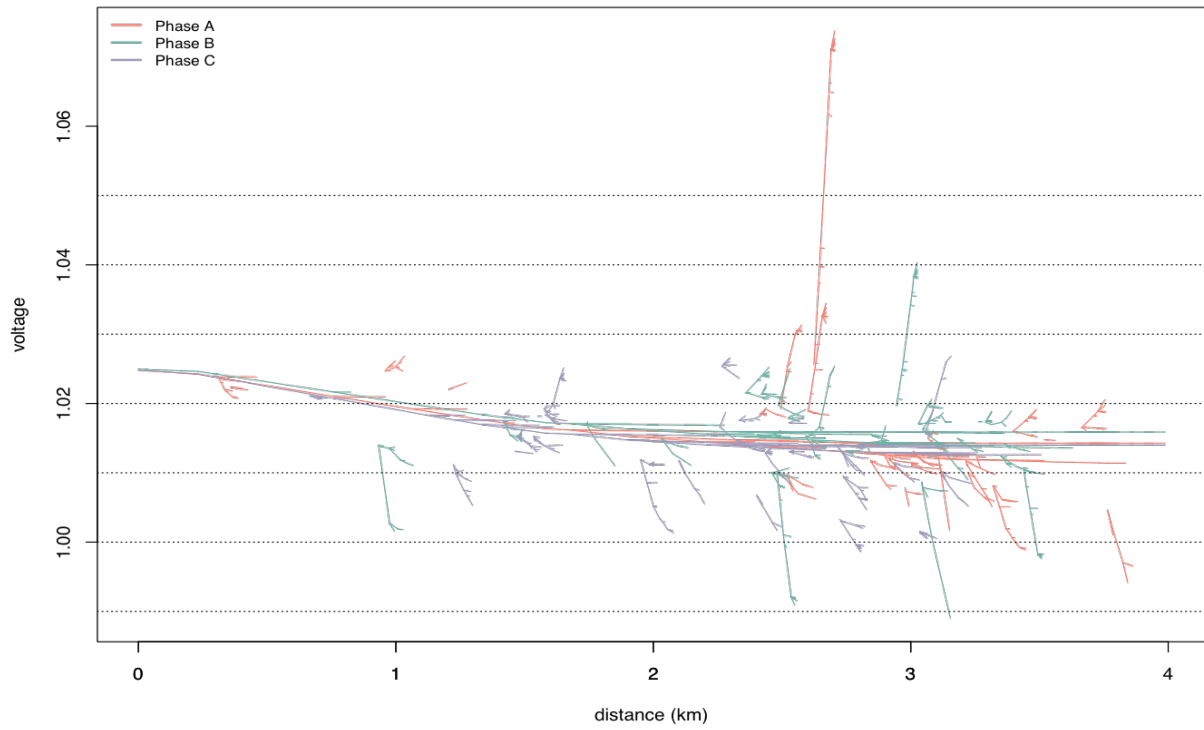


Figure 2.9: Voltage to distance from the substation plot of primary voltages (solid lines) and secondary voltages (dotted lines) for feeder L on May 23 at 12:30 p.m.

Chapter 3

Effectiveness of DER Voltage-Based Grid Support

Functions in Low-Voltage Secondary Circuits

3.1 Introduction

It is becoming increasingly critical to improve the modeling and simulation of customer-end voltages to understand the integration of grid-edge control techniques that leverage the grid-friendly capabilities of customer-sited resource such as advanced inverters in PV systems and load control via HEMS and/or tariff design.

Utility companies across the United States have put considerable effort toward improving the way they represent distribution systems and have sizeable portions of their distribution feeders represented in a commercial distribution software tool. However, these models lack accurate or realistic representations (models) of the low-voltage secondary networks. Utilities are recognizing this limitation and are contemplating the necessary level of detail to capture not only the primary medium-voltages but also the secondary low-voltage level to which PV systems are connected and customers are required to meet requirements. In [38], the authors discuss North American split-phase secondary circuits in detail and compare the full 120 V split-phase models with the single-phase equivalent at 240 V. They find that the load unbalance fully represented in full split-phase models has only a minor influence on the accuracy of the simulated 240 V load voltages and that single-phase equivalent model can be used to accurately represent split-phase secondary circuit 240 V voltages but should not be used to represent unbalanced 120 V load voltages. In [39–42], the authors propose a series of measurements driven methodologies to estimate and validate low-voltage secondary circuits based on AMI and PV system data in a case study on the Georgia Tech Univeristy campus. Reference [43] describes a statistical analysis based on a clustering technique

to represent low-voltage networks out of a large (> 200) sample of designs in the north west of England. This work applies well to 50 Hz systems, but not to 60 Hz systems.

In this chapter, the statistical characteristics of a sample of secondary circuits in Hawai'i that will be used in Chapter 4 to model customer voltages are described, and the effectiveness of voltage-based grid support functions in mitigating the impacts of customer-sited PV systems in secondary low-voltage circuits is also explored.

This chapter is organized as follows: Section 2 describes statistical characteristics of a sample subset of secondary circuits in Hawai'i, and in Section 3 the effectiveness of voltage grid support functions in mitigating secondary circuit voltage rise is described, and finally section 4 concludes and describes future research from this effort.

3.2 Low-Voltage Secondary Circuits and Characteristics from a Sample Subset

To accurately capture the impacts of voltage grid support functions from customer sited resources, it is necessary to represent the voltage rise that will occur across the distribution service transformer and across the conductors to simulate the voltage at the customer site.

For understanding this, real secondary circuit designs from Hawaiian Electric Companies were collected and analyzed. Figures 3.1 and 3.2 show the wide range of electrical distance, in Ohms, in a box-plot representation. This is a standardized way of displaying the distribution of data based on the five number summary: minimum, first quartile, median (red solid line), third quartile, and maximum, with the central rectangle spanning from the first quartile to the third quartile. This illustrates that generalizing a voltage rise across secondary circuits is not very accurate, even within same construction type of overhead or underground designs.

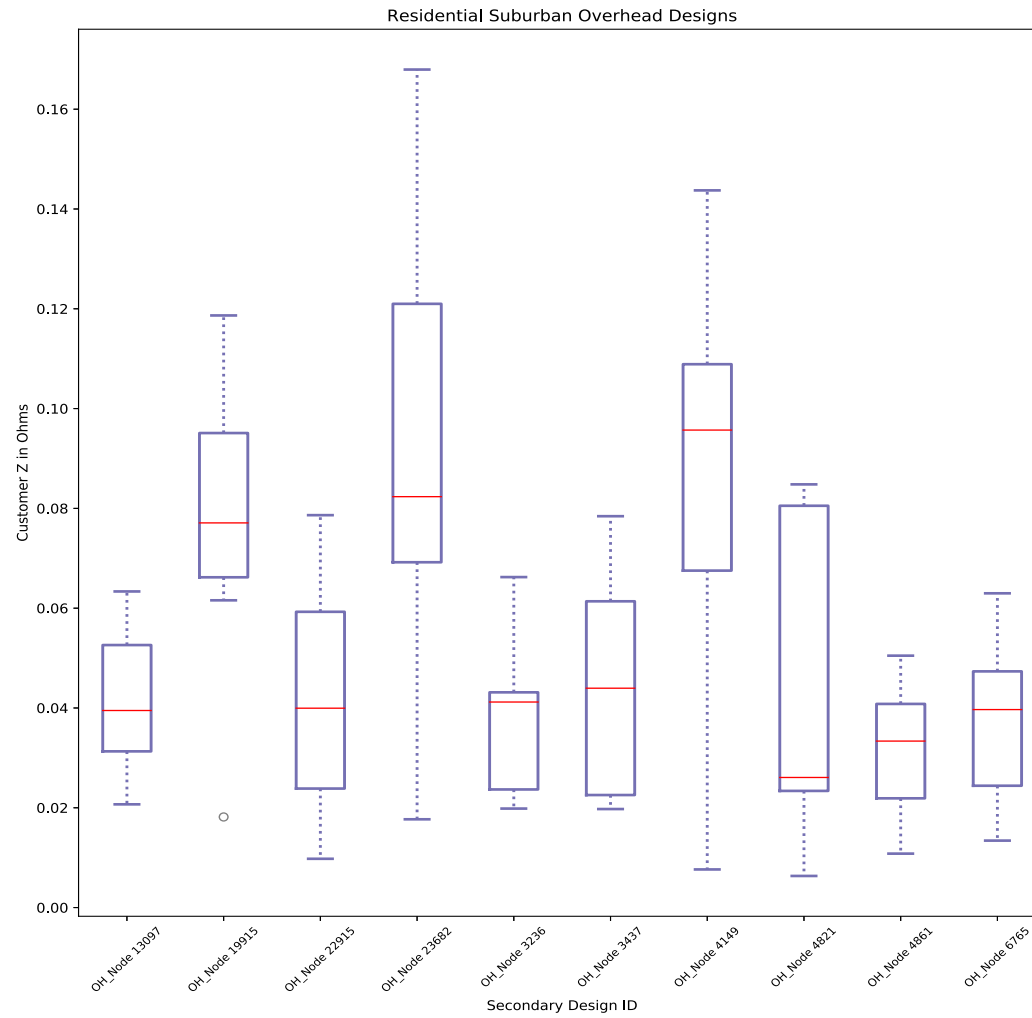


Figure 3.1: Customer electrical impedance for 10 overhead secondary designs.

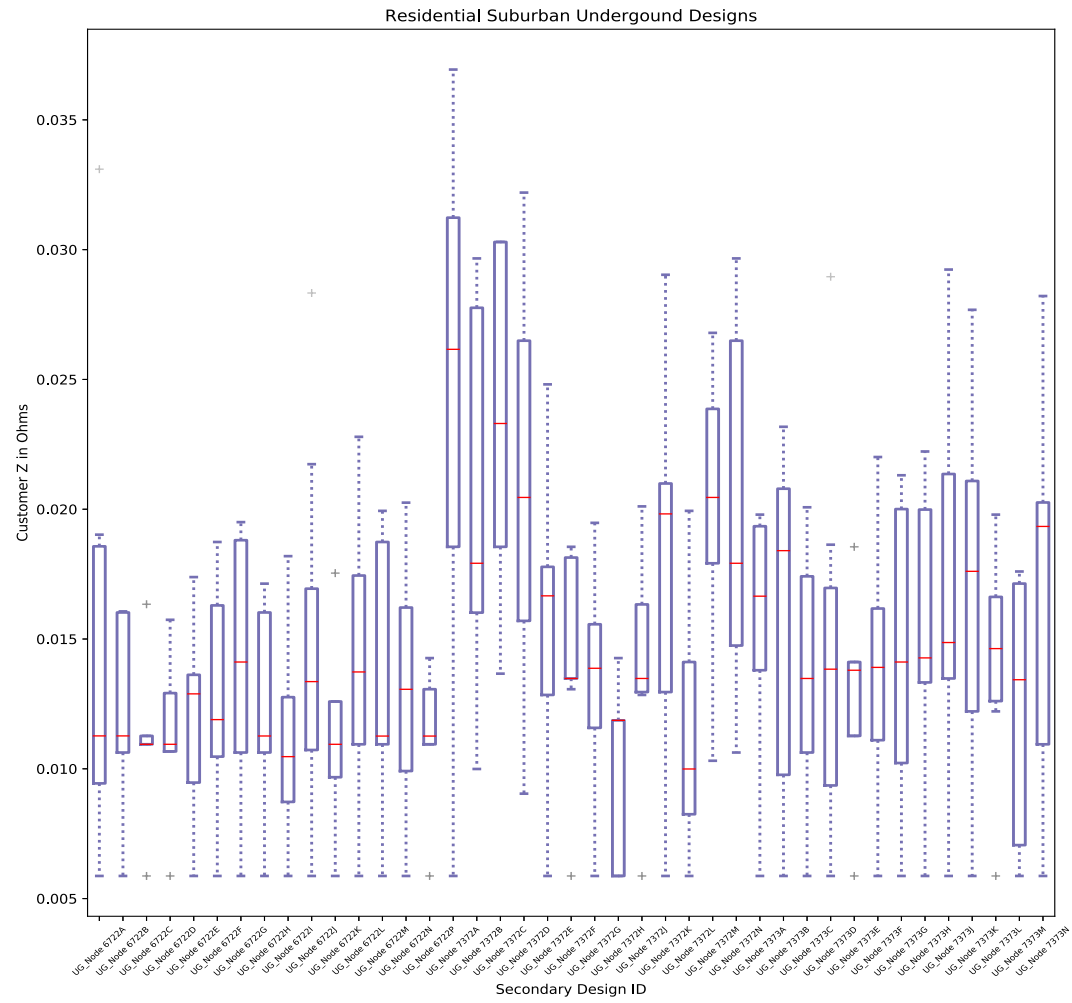


Figure 3.2: Customer electrical impedance for 33 underground secondary designs.

In the next figures, Figure 3.3 and Figure 3.4, a new metric to characterize the degree or level of shared service secondary between customers called "Customer Degree" is proposed. The Customer Degree is defined as the number of customers upstream of a customer on the same branch or shared service. This proposed metric is important because it greatly affects the impact of DERs on voltage rise.

In North America, residential low-voltage circuits are radial, split-phase, with center-tapped service transformer and low-voltage triplex service lines. The challenge is to accurately capture the full split-phase model, active and reactive power measurements from customer side 120 V phases are needed, and this is not currently available from standard utility meters. New AMI meters deployed in the U.S. can measure single-phase real and reactive power (or energy, in kWh) and voltage readings at the 240 V voltage level. So modeling the full 120 V split-phase model with no detailed information on customer unbalanced 120 V phases does not add any accuracy to the single-phase representation of the split-phase model.

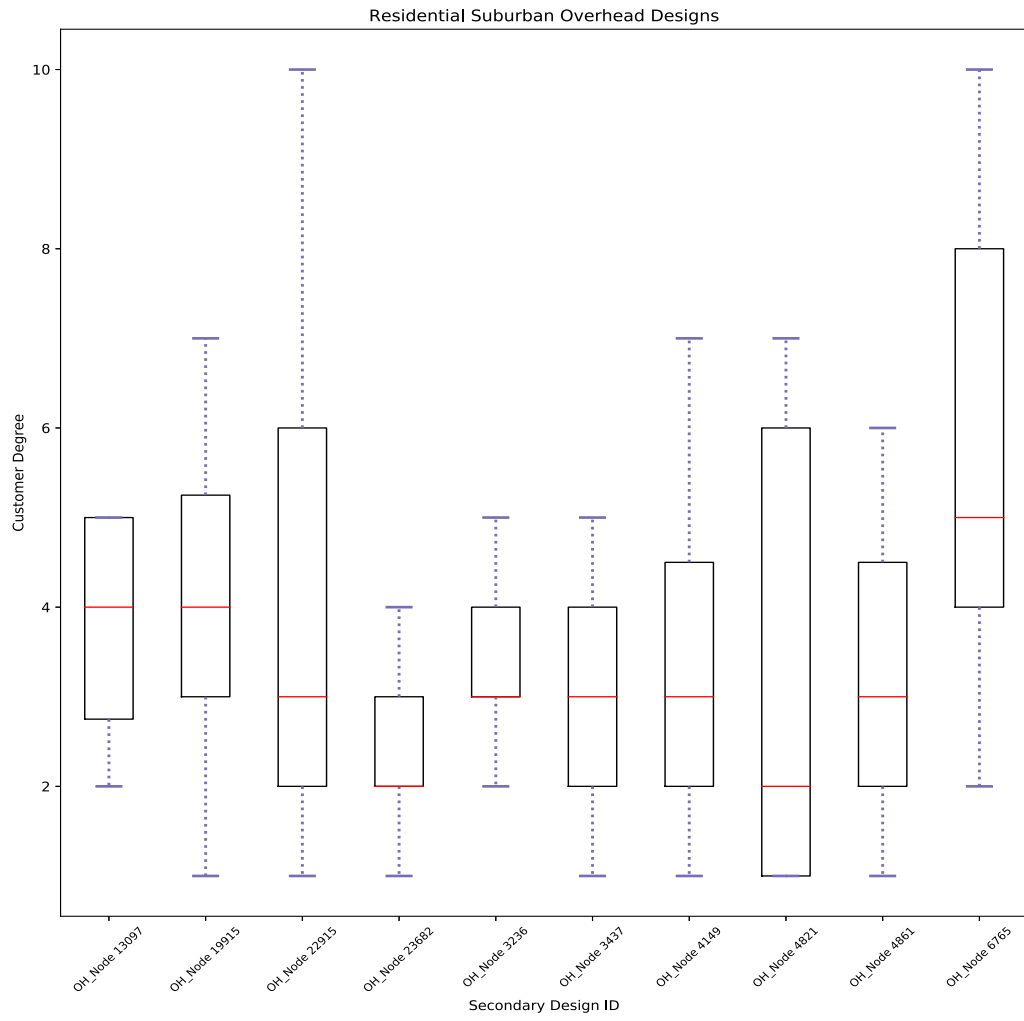


Figure 3.3: Customer degree impedance for 10 overhead secondary designs.

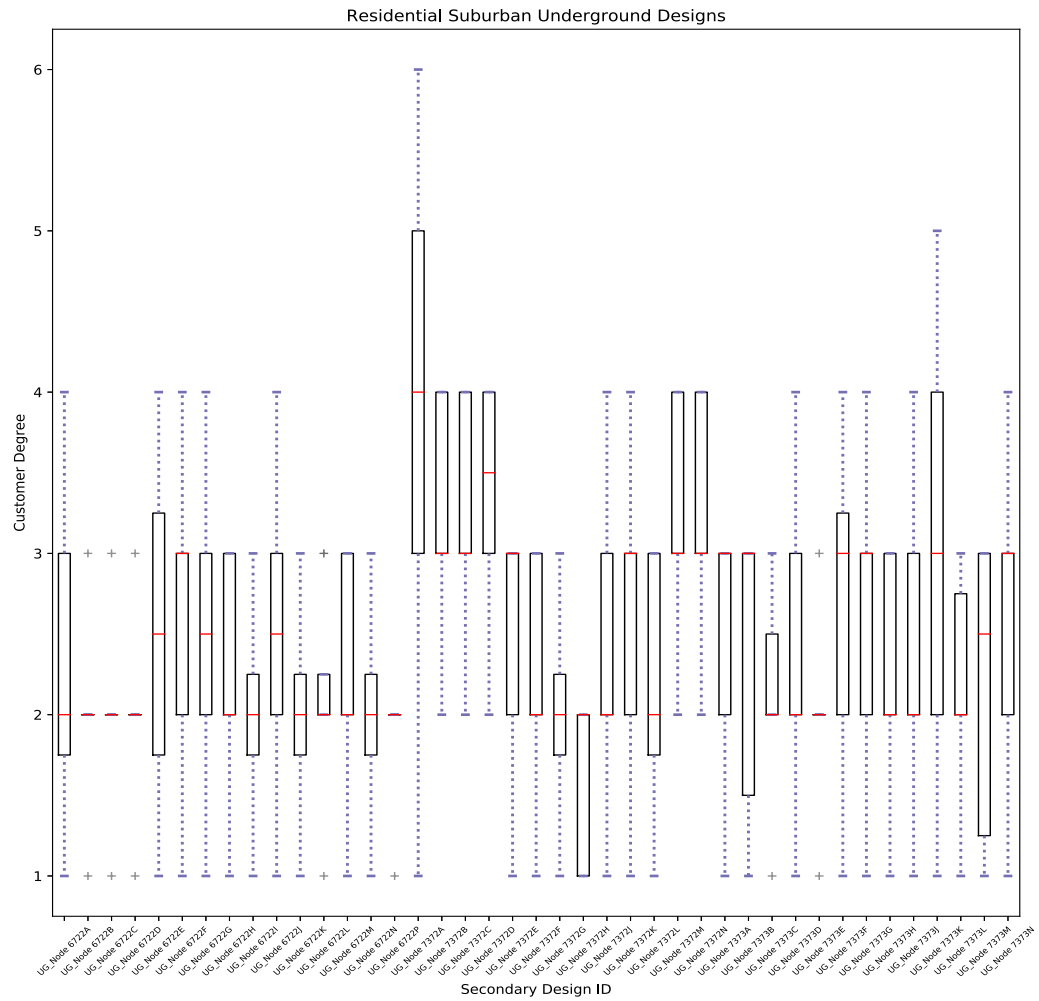


Figure 3.4: Customer degree impedance for 33 underground secondary designs.

Table 3.1: Energy Curtailed from Volt-Var and Reactive Power Absorbed by All Advanced Inverters

Secondary Approximation Method	PV Energy Curtailment	Reactive Power Absorbed
Star Secondaries	32 KWh	485 kVARh
Representative Secondaries	70 kWh	1254 kVARh

3.3 Comparison of Feeder Modeling Results with Representative versus Simplified Secondaries

In this section, the comparison of using a star network design for all customers in the feeder introduced in the previous Chapter 2, versus the more accurate representative secondary designs is described. A star network design is a secondary design in which each customer is connected to the service transformer via a dedicated service feed. In this case, the cable connecting the transformer to the customer is the most commonly used in low-voltage designs, #1/0-gauge cable, and the length is 100 ft.

Figures 3.5 show the voltages for all customers in the M34 feeder using the same star network secondary design downstream all secondary transformers, versus the method for assigning secondaries in this thesis. Figure 3.6 shows the same customer voltages with volt-var programmed in all new inverters. The impacts in the estimation of advanced inverter voltage support and customer impact are non-negligible, as shown in 3.1, the total reactive power support provided by the residential PV systems in volt-var local control mode, and resulting customer energy curtailed. As such, the simplified star design versus the more detailed secondary approximation method presented in this thesis:

- Underestimates PV curtailment due to activation of advanced inverter functions
- Underestimates the reactive power support required from advanced inverters
- Over-estimates the effectiveness of advanced inverter features in regulating voltage

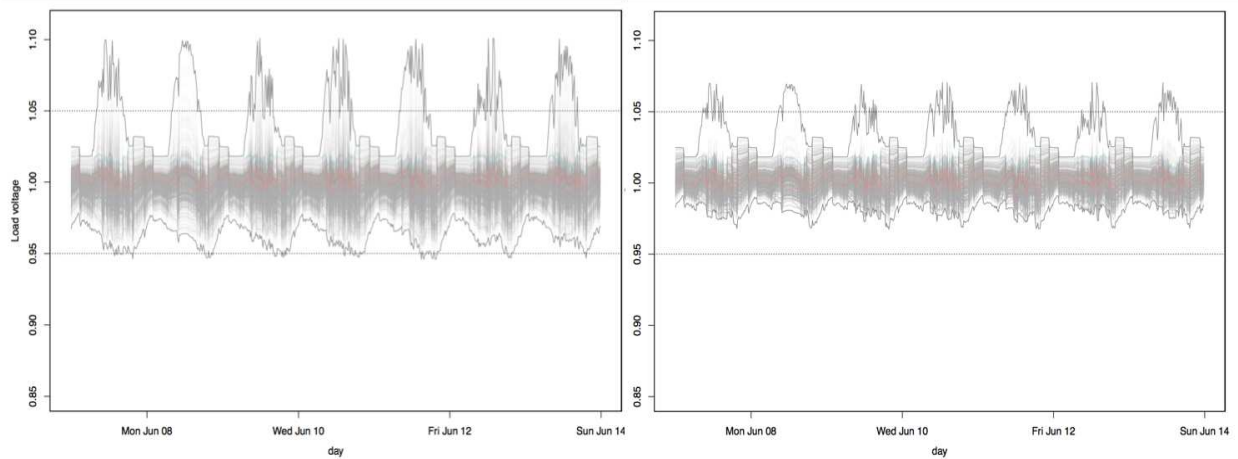


Figure 3.5: Timeseries Voltages for all Customers in Feeder M34 with no Advanced Inverters: a) Representative Secondaries (Left), and b) Star Secondaries (Right).

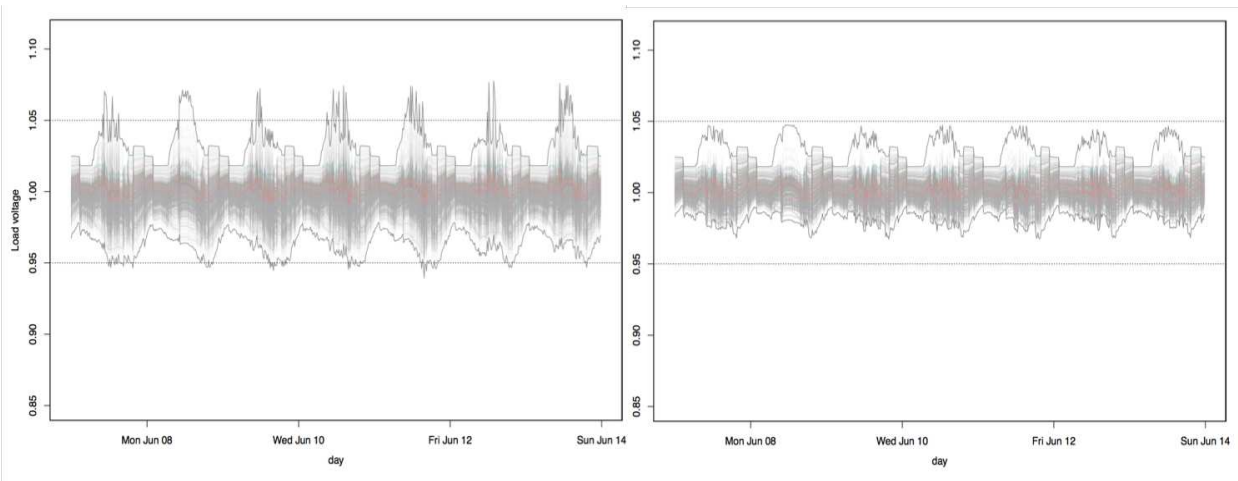


Figure 3.6: Timeseries Voltages for all Customers in Feeder M34 with Volt-Var: a) Representative Secondaries (Left), and b) Star Secondaries (Right).

3.4 Effectiveness of Real and Reactive Power from Customer-Sited DERs for Voltage Support

Utilities are concerned that they may not be capturing accurately in their distribution planning and hosting capacity studies the new DER grid friendly services. This is required in some jurisdictions such as in Hawai'i and California. This work shows that the bulk of the voltage support from advanced inverters absorbing reactive power in constant power factor or volt-var modes is effective at reducing the voltage rise caused by DERs across the distribution service transformer (see Fig-

ure 3.7). The voltage to distance plot of the baseline case, defined here as a high-penetration PV case with all legacy inverters connected at unity power factor, is shown in red. The case in which all of the PV systems, except one, have volt-var activated is shown in blue. It is noticeable how the primary voltage is slightly affected by the effect of volt-var in residential PV customers and that the bulk of the reactive power support provided at the secondary level is effective at reducing the voltage rise across the service transformer. Finally, reactive power support is not effective at mitigating the voltage rise across the secondary conductors. This is due to reactive power being effective where there is a higher reactance component, i.e at the transformer, versus the highly resistive components of the secondary conductors.

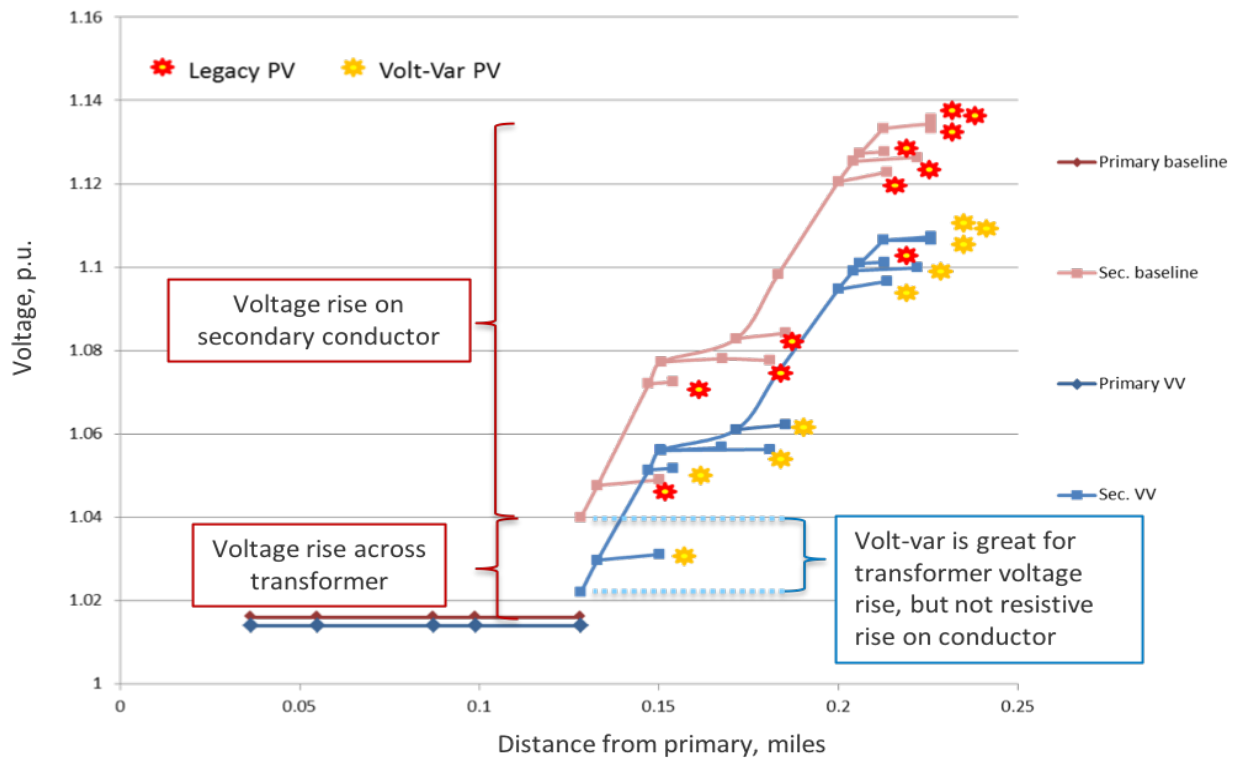


Figure 3.7: Effectiveness of volt-var at reducing voltage rise across a secondary circuit.

3.5 Modeling Low-Voltage Circuits for Hosting Capacity Studies

Hosting capacity is defined as the amount of DER that can be accommodated without adversely impacting power quality or reliability under existing control configurations and without requiring infrastructure upgrades [49]. Limiting factors can be related to voltage violations, thermal violations or protection issues. Voltage is typically the first limiting factor, and presently, hosting capacity studies across the U.S. are performed using primary voltage as the limiting factor to add DERs. The information is then typically made publicly available so that DER developers and customers can review the feeders that may be problematic to interconnect. This can influence the cost of the DER project if upgrades are required or delay the application process due to supplemental reviews.

However, a lot of the PV growth over the past decade has been at the residential and commercial levels, which drives secondary voltages up, but does not greatly affect the primary voltages [34,37]. As such, hosting capacity performed at the primary level only may not capture the effects on local secondary low-voltage circuits that may still trigger delays and costly upgrades to interconnect. Some utilities lower the upper voltage violation limit to account for secondary voltage rise. However, secondary customer voltage rise varies widely and depends on variables such as: construction type (overhead or underground), number of branches, shared main service length, and customers upstream. The concept of hosting capacity could be fully expanded to the secondary low voltage, as proposed in [50]. However, in this case the practical calculation and use of the hosting capacity concept may be compromised by:

- The computation of the hosting capacity at the secondary level which would require secondary low voltage circuit topology and design information, which are typically non-available
- The number of hosting capacity metrics which would increase by several orders of magnitude. Currently the hosting capacity metric is calculated at the feeder level (in the order of magnitude of 100s per utility). The number of hosting capacity metrics would increase

by the number of distribution service transformers per feeder (in the hundreds per feeder), increasing the number of hosting capacity metrics by at least two orders of magnitude.

To capture the effect of advanced inverters in hosting capacity studies, including the distribution service transformer in the power flow of the distribution feeder may be a valid approximation (the full low voltage circuit topology design and customers representation is not necessarily required). Distribution service transformer size and electrical characteristics are information that utilities have, versus the full secondary circuit. Including the distribution service transformer in distribution power flow models does not increase the number of nodes, while including the full secondary circuits increases the number of nodes by at least 3 orders of magnitude (number of lines, and customers per service transformer is at least 10, times the number of service transformers per feeder is in the hundreds).

3.6 Conclusion

In this chapter, the statistical characteristics of a sample of secondary circuits in Hawai'i are described to show the importance of further exploring low-voltage circuit topology. The effectiveness of voltage-based grid support functions in mitigating the impacts of customer-sited PV systems is also explored to show where along the medium and low-voltage circuits is active and reactive power effective at reducing voltage rise. Reactive power support is effective at reducing the voltage rise across the service transformer due to its high reactance value; however, reactive power is not effective at mitigating the voltage rise across the highly resistive secondary conductors.

Chapter 4

Impacts of Voltage-based Grid Support Functions on the Utility and the PV Customers³

4.1 Introduction

Increasing levels of distributed energy resources (DERs) located at or close to the customer site is changing the way the power system, and in particular the distribution system, is planned and operated. Not only are power flows in the distribution systems now bidirectional, but DERs are able to provide grid support functions (GSFs) such as voltage and frequency support [32]. Utilities are increasing their efforts to include DERs in planning and operation. At the distribution level, utilities are looking at the impact of autonomous voltage-based GSFs such as volt-var and volt-watt in voltage regulating strategies, as well as impacts on energy production for customers that are activating such functions [28].

The newly revised IEEE 1547-2018, titled "Standard for Interconnection and Interoperability of Distributed Energy Resources with Associated Electric Power Systems Interfaces" includes advanced specifications for DERs, particularly related to reactive power capability and autonomous voltage/power control requirements impacting the local distribution system to which they are interconnected. Curtailment of active power is required if necessary to meet the apparent power constraints while injecting or absorbing reactive power at up to 44% of the nameplate kVA rating [25]. Reference [51] describes the topology, characteristics, and simulation-based results of an advanced inverter designed to look beyond the recommendations of the previous version of the IEEE Standard 1547 (2003) by including reactive support function.

Inverter voltage support GSFs are activated to mitigate possible off-nominal voltage conditions including over-voltage violations outside of the allowable ANSI C84.1 Range [4], including those

³This chapter is published in [45] and the copyright is included in Appendix A.

contributed to by DER integration. However, these GSFs can cause energy curtailment to photovoltaic (PV) customers. For instance, advanced inverter controls allow PV - inverter systems to support reactive power priority by curtailing active power output when required to keep the grid within its operational constraints [33].

In [37], techniques to create distribution models for determining the effectiveness and impacts of various GSFs were presented. There we leverage such distribution models to present the results of running time-series distribution models with different penetration levels of DERs.

The authors in [33] argue that there is no obvious nexus between increased reactive power output and decreased PV kWh generated and show that the application of volt-var control could mitigate voltage violations without causing PV active power curtailment. Reference [31] investigated the impacts of various penetration levels of advanced inverters on a typical distribution network showing that smart inverters have the capability to improve tap operations, voltage variability, and minimum and maximum voltages. Reference [32] presented a methodology for the optimal settings of a group of advanced inverters using autonomous inverter control (i.e., an inverter output is a function of its primary node at the point of connection). The study revealed that optimal settings depend on inverter kVA rating, feeder layout, load and solar characteristics. A method to design a smart inverter volt-watt control to mitigate possible voltage violation for a high PV penetration case while curtailing energy evenly among all integrated PV systems is presented in [36]. Other related studies in [52], [53] present the use of advanced inverter settings to enhance grid performance.

However, to the knowledge of the authors, the extended literature has not characterized and quantified or estimated the expected level of energy curtailment as a result of the activation of volt-var in combination with volt-watt. Our study proposes four metrics—maximum GSF and average GSF curtailment, average increased generation and average net generation change—to assess the full impact of a given GSF control on customer-sited PV systems. We then apply those metrics to several detailed quasi-static time-series (QSTS) simulations of a distribution feeder with various levels of PV generation. Finally, we plot curtailment of customer PV generation as a function of

peak customer voltage and demonstrate a tight and predictable relationship between the two. This relationship is leveraged to make recommendations for how utilities may take advantage of the benefits of volt-var and volt-watt control without significantly impacting customer PV generation and without investing in irradiance sensor deployment or advanced analytics to estimate curtailment. These findings align with field measurements of PV systems performing volt-var and volt-watt control on several distribution circuits with high levels of distributed PV on Oahu, Hawaii, as described in [54].

The rest of this paper is organized as follows: section II describes some voltage-based GSFs, metrics, and impacts; case studies are presented in section III and the results are discussed in section IV; and section V concludes.

4.2 Voltage Based Grid Support Functions, Metrics and Impacts

Active-power production from DERs tends to increase steady-state grid voltage, specially in secondary distribution circuits. Inverters, which are the most prevalent power electronics technology due to the popularity of PV systems in customer rooftops, have two output parameters available to mitigate this: reactive power and active power. Absorbing reactive power can bring down voltage with minimal (sometimes zero) impact on real power production and, hence, is generally preferred. Reducing active power can also mitigate overvoltage, but this directly reduces PV energy production and is, therefore, typically considered an option only when voltage is very high and reactive-power management does not solve the problem.

4.2.1 Two voltage grid support functions

In the volt-var control mode, reactive power is modulated in proportion to voltage deviation, absorbing and injecting reactive power or volt-ampere reactive (VARs) for high and low voltage scenarios, respectively. This is done by following a volt-var curve, which often has a deadband where reactive-power production is zero as shown in the top of (Figure 4.1). The volt-var curve

studied in this paper corresponds to a moderate curve with a deadband of $\hat{A} \hat{s} 0.03$ p.u., and a droop curve above 1.03 and below 0.97 p.u.. The droop slope reaches full reactive power injection and absorption at 1.06 p.u. and 0.94 p.u., respectively. Full VARs are defined as 44% of the inverter apparent power rating which corresponds to power factor of 0.9 at full apparent power. The full reactive power capability, however, only is used when the voltage is far from nominal.

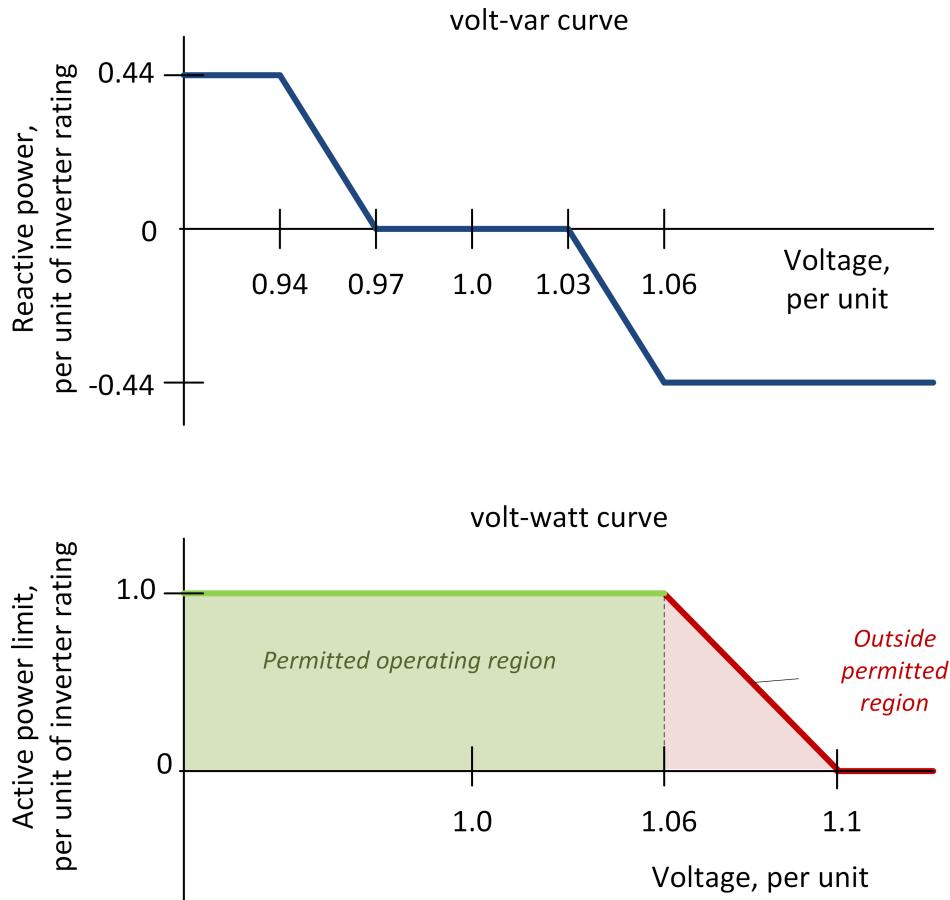


Figure 4.1: The two voltage grid support functions and the settings used in this study

Under volt-watt control, active power is reduced for high voltages to remain on or below a volt-watt curve as shown in the bottom portion of (Figure 4.1). The volt-watt function initiates reduction in real power when the voltage at the point of common coupling (PCC)—not necessarily the inverter terminals—breaches 1.06 p.u.. ANSI C84.1 Standard provides that voltage delivered

at the PCC should generally be within ± 0.05 p.u. of the nominal value. So volt-watt provides means to protect utility voltages from greatly violating ANSI C84.1 service voltage ranges.

4.2.2 Volt-var in reactive and active power priority modes

Reactive power-based functions such as volt-var control can be configured to prioritize either active or reactive power when the inverter's current limit does not allow it to produce the desired amount of both P and Q simultaneously. This is illustrated in Figure 4.2. Active power priority (Watt priority) can be used to ensure zero impact on energy production when providing reactive-power support to the grid. This was briefly called for in California Rule 21; however, active power priority causes grid support to be unavailable during times of high PV production, when voltage control is most needed. For this reason, the IEEE Standard 1547-2018 revision requires reactive power priority.

Reactive power priority (Var priority) mode is required to allow DERs to supply or absorb reactive power when available up to 44% of the nameplate KVA rating for maximum VAR injection and absorption at rated DER voltage [25]. However, enabling the VAR priority mode can lead to active power curtailment as shown in 1-3: For a given PV system, the available active power with volt-var in VAR priority mode, $P_{VV\text{ar},V\text{ar}}$, is

$$P_{VV\text{ar},V\text{ar}} = \sqrt{(S_{inv})^2 - (Q_{VV\text{ar},V\text{ar}})^2} \quad (4.1)$$

where S_{inv} and $Q_{VV\text{ar},V\text{ar}}$ are the inverter capacity (kVA) and reactive power, respectively. The VAR priority mode will result in P_{curt} curtailment if the inverter capacity is not large enough to provide reactive power support based on the droop curve [33], [53].

The reactive power priority illustrated in Figure 4.2 shows that the possible curtailment of available active power to meet the required reactive power as specified by the VAR priority mode. The active power curtailed P_{curt} shown in Figure 4.2 is given as:

$$P_{curt} = P_{VV\text{ar},Watt} - P_{VV\text{ar},V\text{ar}} \quad (4.2)$$

where $P_{VVar,Watt}$ and $P_{VVar,Var}$ are the available active power in active and reactive power priority modes respectively.

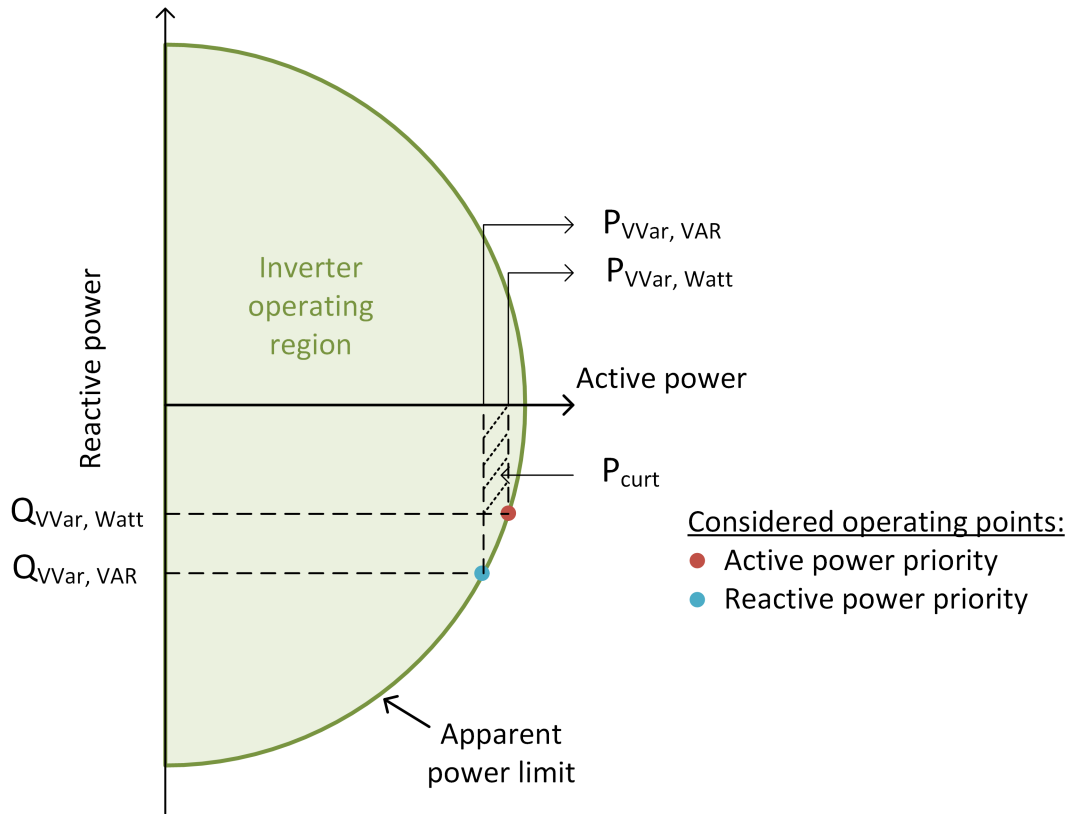


Figure 4.2: Volt-var reactive power and active power priority modes

4.2.3 Impacts of grid support functions

From the perspective of the distribution utility, any voltage-based GSF initiated by the DER will impact distribution system voltages. Reference [34] shows that most of the local reactive power based voltage control effectuated by DERs affects voltage magnitudes across the secondary of the service distribution transformer since it is the portion of the secondary circuit with higher reactance values (when compared to secondary conductors which tend to be dominated by the restive component of the impedance), and as such is affected by the production of reactive power by DERs. Primary feeder voltages are not highly affected by local voltage support by smaller

customer-sited DERs, and the utility voltage-regulating equipment is not typically affected by these local voltage support functions.

From the perspective of the customer, voltage-based GSFs from the DERs can impact the energy production since the active power output of the inverter may be reduced during GSF actions. We focus on quantifying impacts of GSFs on energy production from customer-sited PV installations.

4.2.4 Metrics

The metrics proposed in this paper are related to the impact of a given GSF control on residential customers:

- *Max GSF curtailment* is the maximum customer energy curtailed over a given time period.
- *Average GSF curtailment* is the average customer energy curtailed over a given time period.
- *Average increased generation* is the average customer increased energy generation at the customer site for a given time period because resulting from reduced PV inverter disconnections for voltages above 1.1 p.u. With volt-watt activated, some PV systems continue to produce when they otherwise would have been disconnected at 1.1 p.u..
- *Average net generation change* is the average customer increased generation minus the average grid-support function curtailment for a given time period. A positive value represents a net increase in PV generation.

To calculate the energy curtailed due to voltage-based GSFs in DERs, the baseline scenario with no GSF must be established first. Similarly, to calculate the increased generation metric, the scenario with no disconnection for voltages above 1.1 p.u. must be studied first.

4.3 Test Feeders, PV Penetration Cases and Grid Support Function Scenarios

Here we present the distribution feeder, the PV penetration cases, and the GSF scenarios studied to quantify the impacts of voltage-based GSFs on the energy production at PV installations located at customer sites.

Substation M34 located in Oahu, HI, has two 12 kV distribution circuits. This test system was selected for its diversity of the different types of PV installations already existing on a circuit (e.g., residential, commercial, and large feed-in-tariff (FIT) projects) that are rated at approximately 500 kW each. For more information on the feeder model preparation for QSTS simulation of this test system with detailed secondary circuit approximation, see [37]. The scenarios described below are run at 15 min time-steps.

To create various levels of penetration of PV in the test system, calculated with respect to the gross daytime minimum load (GDML), blocks of approximately 1.6 MW of residential PV projects are added to the baseline feeder. Note that the baseline feeder already has 7 MW of large primary connected PV systems and 3.4 MW of residential PV, all connected at unity power factor. The scenarios shown in Table 1 were run for a week in June with incidences of high voltages.

Scenarios 1a and 1b are not expected to occur in the future since volt-var is a requirement for DER interconnection in Hawai'i Rule 14H, but they are run to establish a baseline for PV production without advanced inverter functions, and obtain the baseline production of PV systems without GSFs. Scenarios 2a and 2b are studies to show the effectiveness and impact to energy production of enabling volt-var in all new residential PV systems added. These can be compared to scenarios 3a and 3b, which model blanket activation of volt-var in combination with volt-watt (volt-var-volt-watt) in all new residential PV systems added to the 2016 baseline. Comparing scenarios 2a and 2b with 3a and 3b will provide insight into how much the volt-watt function is activated when implemented in combination with volt-var.

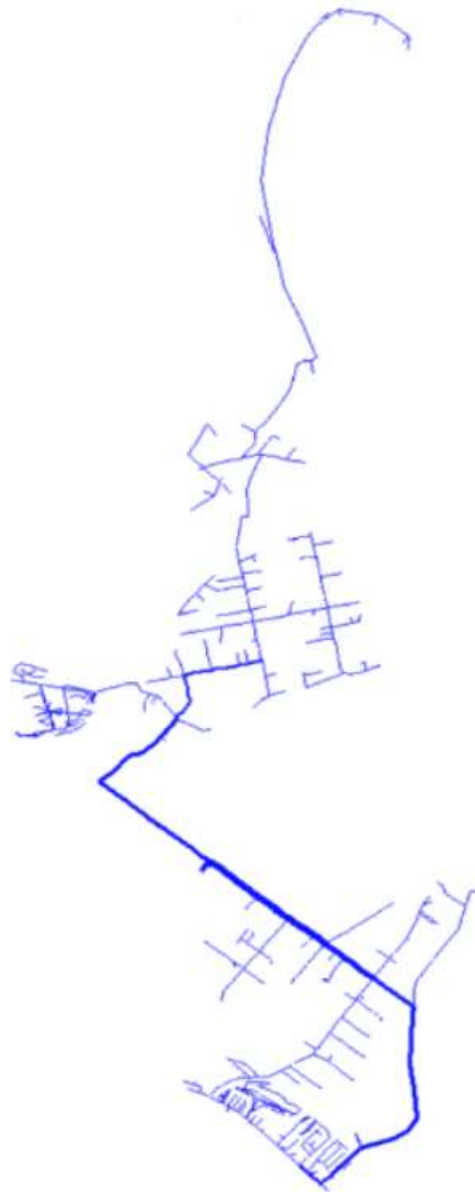


Figure 4.3: Geographical view of M34 distribution feeder

Note that the difference between scenarios "a" and "b" is that in the former PV systems do not disconnect when they sense voltages above 1.1 p.u., and in the latter they do, per IEEE 1547. Studying scenarios without disconnection above 1.1 p.u. enables the calculation of the increased generation metric that quantifies the PV systems that are able to produce more energy because they are no longer tripping at 1.1 p.u. voltage magnitude. This simulation does not capture the interactions that may occur in the real world at time-steps less than 15 min, and assumes that the

Table 4.1: Scenario Description for M34 Feeder at various GDML PV Penetration Cases

2*S/N	2*Scenario	PV Penetration with GSFs		
		175% "Low"	370% "Medium"	600% "High"
1a	PV-No GSFs-n/D	2* 1.86MW at PF = 1	2* 3.5MW at PF = 1	2* 5.3MW at PF = 1
1b	PV-No GSFs-w/D			
2a	volt-var-n/D	2* 1.86MW in volt-var	2* 3.5MW in volt-var	2* 5.3MW in volt-var
2b	volt-var-w/D			
3a	volt-watt-n/D	2* 1.86MW in volt-watt	2* 3.5MW in volt-watt	2* 5.3MW in volt-watt
3b	volt-watt-w/D			
n/D = no disconnect; w/D = with disconnect (inverters disconnect if V > 1.1 p.u.)				
There are 3.4 MW of rooftop and 5.2 MW FITs legacy PV systems connected at unity power factor.				

inverters are on or off the entire 15 min time period. In reality, inverters would wait for measuring 5 minutes of steady-state voltage below 1.1 p.u. to reconnect to the grid.

4.4 Results of High-Penetration PV Cases with Residential volt-var (VV) and volt-var-volt-watt (VV-VW) GSFs

4.4.1 Customer Energy Production Metrics

Table 4.2 shows the proposed calculated metrics for a high voltage week in June for three increasing PV penetration levels. The maximum customer curtailment in volt-var mode remains at 1.8% and is independent of the PV penetration level. However, for the volt-var-volt-watt mode, the maximum customer curtailment increases rapidly from 2.3% in the low PV penetration case to 5.7% in the high PV penetration. Yet, the average customer energy curtailment values are the same or slightly lower in the volt-var-volt-watt case, than in the volt-var alone scenario. This suggests that very few customers experience non-negligible volt-watt GSF activation, and that the effectiveness of volt-watt in lowering voltages for a few outlier customers slightly lowers the curtailment for the remaining of the customers that experience only volt-var activation.

Table 4.2: Impact of activating GSF control on PV systems and energy curtailment at different penetration levels

3*Metrics	GDML penetration levels					
	175%		370%		600%	
	VV	VV-VW	VV	VV-VW	VV	VV-VW
Max GSF Curt.	1.8%	2.3%	1.8%	3.7%	1.8%	5.7%
Ave. GSF Curt.	0.10%	0.07%	0.15%	0.13%	0.24%	0.23%
Ave. Incr. Gen.	2.1%	2%	2.7%	2.6%	2.7%	3%
Ave. Net Gen.	2%	1.9%	2.5%	2.4%	2.4%	2.8%

The other metric proposed in this paper is the increased energy generation that is no longer lost due to disconnecting above 1.1 p.u. per IEEE 1547. The increased generation increases the higher the PV penetration is. This is expected since the more rooftop PV, the higher the voltages are, and as such more PV customers are pushed above 1.1 p.u., and so with grid support functions reducing voltages, more generation is lowered below 1.1 p.u. and is able to generate.

The net generation change—which is positive if there are more PV customers enabled to generate than curtailed for the GSFs—is positive for all the scenarios studied. The net generation change increases considerably between the low and medium PV penetration levels. However, as the PV generation increases between the medium and the high PV penetration case, the net generation change stalls since as there is more energy curtailed too.

4.4.2 Customer Energy Curtailment versus Maximum Customer Voltage

These findings are illustrated by plotting the customer energy curtailment values against the maximum voltage experienced by the customer. Each dot in Figures 4.4 – 4.6 represents a customer, with blue and pink dots representing VV and VV-VW. In the low PV penetration case, very few customers experience the activation of volt-watt when combined with volt-var. As PV penetration increases, more customers have volt-watt activation, but still less than 10 customers out of 531 PV systems are affected by this activation in the very high PV penetration case.

These plots also show that the energy curtailment is negligible even for the very high penetration case provided peak voltages are within the ANSI C84.1 range. The utility can leverage

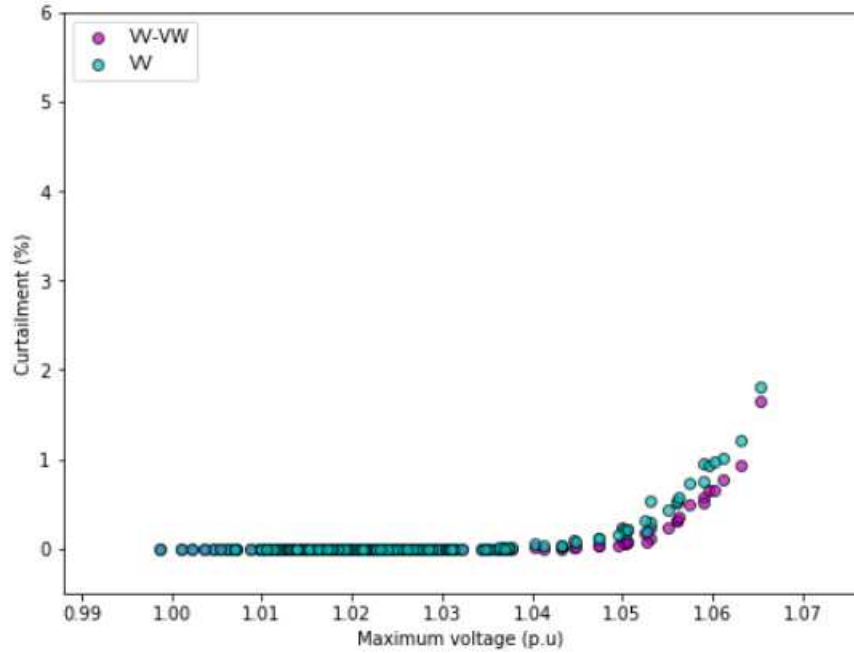


Figure 4.4: Weekly customer energy curtailment versus maximum voltage for the low PV penetration case

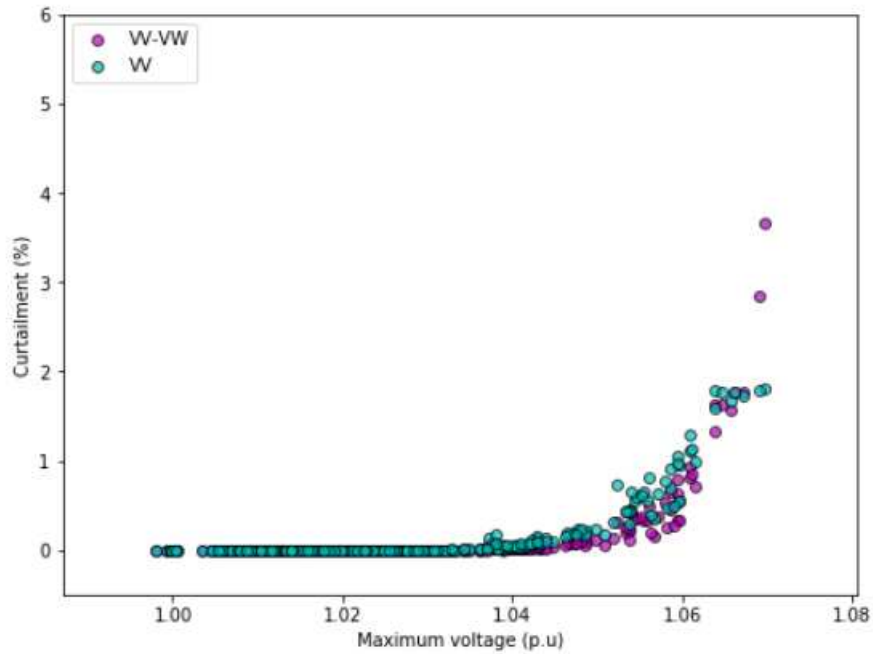


Figure 4.5: Weekly customer energy curtailment versus maximum voltage for the medium PV penetration case

this because voltage violation problems may point to possible curtailment issues, which require appropriate mitigation measures. Consequently, the concerned service provider may want to pro-

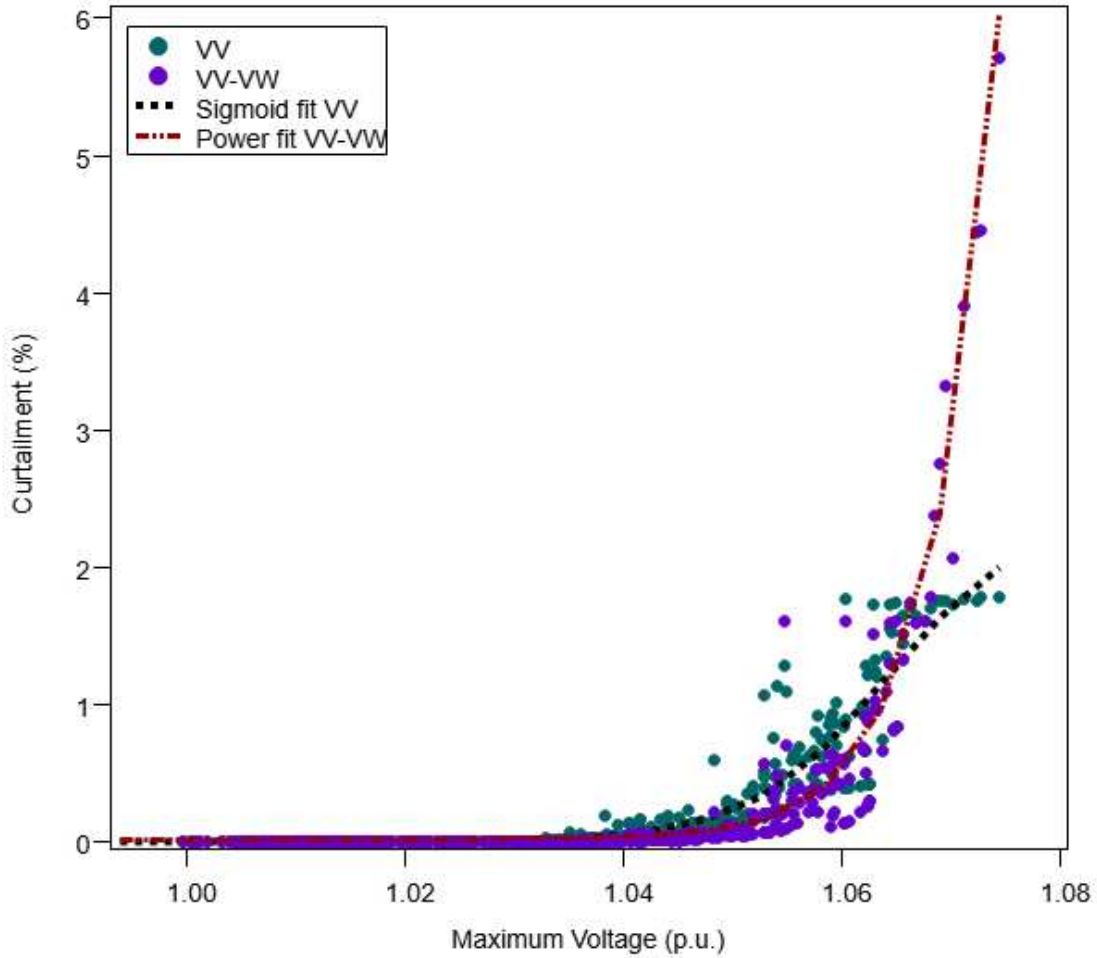


Figure 4.6: Weekly customer energy curtailment versus maximum voltage for the high PV penetration case. This figure illustrates the relationship between maximum voltage and curtailment for two scenarios: VV (green dots) and VV-VW (purple dots). The VV curve follows a sigmoid function with a plateau that accounts for the reactive power limit (0.44 p.u.) of the VV curve; while a power fit function converged properly for the VV-VW scenario. Voltage violation mitigations would address both curtailment and voltage issues.

In addition, we have added curve fitting functions to Figure 4.6 for the high penetration PV case for the VV and VV-VW scenarios. The VV curtailment versus maximum customer voltage curve follows a sigmoid function with a plateau that accounts for the reactive power limit (0.44 p.u) of the VV curve; while a power fit function converged properly for the VV-VW scenario. The utility could use these curve fitting functions to estimate customer curtailment based on peak voltage. This will be further explored in future work.

4.5 Conclusion

We propose four new metrics for quantifying the impact of voltage-based GSFs to customer energy production, and provide results for three PV penetration cases for a high voltage week-long simulation on a 12 kV feeder in Oahu, HI. The metrics show that the activation of voltage-based GSFs, such as volt-var and volt-watt, results in a positive average net generation change, since there is less energy curtailed due to the activation of the GSFs than there is generation prevented from tripping above 1.1 p.u. per IEEE 1547. We also propose a new curve for plotting the customer energy curtailment versus customer maximum voltage, which shows that when customer peak voltages are maintained close to the ANSI C84.1 recommendations, customer energy curtailment from GSFs such as volt-var and volt-watt will be negligible or very low. These findings align with the limited field measurements available in [54].

Chapter 5

Estimation of Solar Photovoltaic Energy

Curtailment Due to Volt-Watt Control⁴

5.1 Introduction

As the pace of the current energy transition continues to increase rapidly, demand for clean energy supply, policy support for renewable energy, reduced technology costs, and high penetrations of variable generation pose new challenges to the reliable operation of the electric grid [56–58].

Utilities are adopting various strategies to mitigate the adverse impacts (such as steady-state overvoltage issues) of increasing integration of distributed energy resources (DERs) with the power system. Some measures include conventional methods such as configuring load tap changer settings and upgrading secondary conductors and distribution transformers. Another mitigation option is the use of nonwire alternatives, such as distributed static volt-ampere reactive (VAR) compensators, energy storage, advanced load controls, coordinated DER controls, and autonomous inverter-based solutions [59–61].

The current near-term solution prevalent in the study location, Hawaii, however, is the activation of smart inverter-based voltage regulation controls. Hawai'i has more distributed photovoltaic (PV) than any other U.S. state as a proportion of the load, and DERs plays a significant role in the state's plan for 100% renewable energy by 2045. The proliferation of autonomous inverter-based solutions to mitigate persistent voltage excursions caused by high-penetration PV systems has drawn increasing interest in their impact on customer solar energy curtailment. Some impacts of curtailment include a decrease in PV capacity factors, an increase in the levelized cost of energy, and a decrease in avoided fossil fuels [62].

⁴This chapter is published in [55] and the copyright is included in Appendix A.

It is now important to quantify the amount of PV energy curtailed as a result of the activation of inverter-based grid support functions (GSFs) to assess performance and potential incentives or compensation mechanisms [63]. From the regulator and utility perspectives, as customer-sited resources are used to provide localized voltage support, it is important to estimate the potential impact to the customer's energy production. From the customer and solar developer's perspectives, estimating the potential curtailment is important to account for in the economic valuation of DER projects. There seems to be a growing interest among utilities, PV industry stakeholders, and regulators, for a low-cost, widely deployable methodology for estimating potential curtailment.

This is challenging because of the difficulty for a PV system that is not operating at its present maximum available power to know what its present maximum available power is in real time [64]. The extant literature proposes various offline methods for maximum point estimation using regression analysis or neural networks, which may require a very high processing power more than what a typical PV inverter's embedded processor can handle [65,66]. Real-time estimation methods make assumptions that can impact the accuracy of the PV model or may require information that is not typically available on PV module data sheets [67,68].

A few studies in the extant literature have investigated the impact of GSF activation on PV energy curtailment, mostly by providing simulation-based curtailment estimates. Seuss et al. used the voltage at the point of common coupling (PCC) to estimate PV energy curtailed, where curtailment was performed by ramping down PV active power depending on the voltage measurements in a volt-watt droop [69]. This method required deploying an additional controller at the PCC, and the sensitivity of the PCC voltage to the network impedance as seen by the inverter could affect the accuracy of the measurement.

Latif et al. quantified curtailed energy by calculating the difference between the inverter active power output and maximum active power point [70]. Curtailment estimation based on inverter production data would require a system-wide deployment of communications infrastructure to capture and relay data to system operators. Kashani et al. proposed a method to design volt-watt control

parameters to maximize the benefit of such control application while evenly distributing the weight of PV energy curtailment [36].

Shuvra et al. proposed a dynamic smart inverter voltage support strategy for a two-stage PV inverter architecture, that can be applied to various feeders with different X/R ratios. However, such control strategy could have an impact on PV production and therefore, the quantification of the potential curtailment caused by this control application becomes pivotal [71].

Nassif et al. investigated the impact of the volt-watt function on PV curtailment and voltage management with the installation of a battery energy storage system on a the feeder in a Canadian electric utility. The study showed that with the deployment of an energy storage system, the PV output could change without any constraint because the storage levels off PV production [72]. None of the existing literature summarized above presents a method for estimating PV curtailment from volt-watt control without additional sensors or communications. Other related studies have considered only the performance and effectiveness of smart inverter GSFs in mitigating voltage issues on the distribution network [73–79].

The extant literature shows the implementation of smart inverter GSFs mainly through simulation studies, without actual field validations. Also, a considerable number used the primary voltage level of the distribution network, without taking into account the unique secondary network topology. Through collaborative engagements, the National Renewable Energy Laboratory and Hawaiian Electric have performed a more detailed distribution modeling effort—from the primary voltage level down to the customer premises—to capture the full impacts of customer-sited autonomous inverter control.

In a previous voltage regulation operational strategy (VROS) study by the authors [35], PV energy curtailment was estimated using a detailed simulation for hundreds of customers in Hawai'i with rooftop PV and advanced inverters. Curtailed PV production was estimated by computing the difference between a base case scenario simulating customer PV output without GSF activation and a scenario with GSF activation in a time-series power flow simulation. The study revealed that the impact of volt-watt control on PV energy production is typically negligible (less than 2% for most

customers) when activated in combination with volt-var. In rare cases with voltage persistently or frequently above 1.06 p.u., volt-watt control could result in non-negligible curtailment. In such cases, the utility has a preexisting obligation to maintain voltages within ANSI range [4] and fix the voltage issue, which also mitigates high volt-watt curtailment.

Some methods available to utilities include replacing neighbors' legacy inverters with smart inverters, applying more aggressive volt-var curves, using volt-watt (potentially compensating a customer for lost production), or a combination of all of these. For volt-watt application, however, there is a need for a reliable estimate of lost production without incurring additional costs—for example, the cost of additional sensors and communications infrastructure to transfer inverter data to utilities.

The main contributions of this paper are as follows:

- This paper proposes a methodology for estimating PV energy curtailment caused by volt-watt control using only smart meter voltage data, without the need for additional sensors, communications, or inverter data. This method assumes maximum possible curtailment for a given volt-watt curve based on the smart meter voltage during the time period of interest.
- This study compares the proposed methodology with actual field measurements using irradiance sensing and inverter data in Hawai'i and with data from a previous simulation-driven study on the impact of advanced inverter GSF activation on PV energy curtailment.

The remainder of this paper is structured as follows: Section II summarizes autonomous inverter-based volt-watt control. Section III presents the proposed method for estimating PV energy curtailment from smart meter voltage and also summarizes the method for measuring curtailment from irradiance and inverter data. Section IV presents methods for evaluating curtailment estimates. Section V presents the performance evaluation of the proposed methodology. Finally, Section VI concludes.

5.2 Autonomous Inverter-Based Volt-Watt Control

This study considers estimating curtailment only from the volt-watt advanced inverter functionality. In Hawai'i and other U.S. regions, such as California, volt-watt is implemented in combination with volt-var control. Figure 5.1 shows Hawaiian Electric's approved volt-var and proposed volt-watt curves. The volt-var curve has a deadband of ± 0.03 p.u. and a droop slope $\Delta Q/\Delta V$ of 14.7. The droop curve at 0.94 p.u. and 1.06 p.u. reaches full VAR generation (positive VAR) and absorption (negative VAR), respectively. The inverter is required to prioritize VAR production or absorption over active power production. Full VARs are defined as 44% of the inverter nameplate capacity, which corresponds to 0.9 power factor at full apparent power.

The volt-watt curtails the active power output as voltage exceeds 1.06 p.u., as shown in Figure 5.1. Volt-watt control serves as a protection against occasional voltages outside ANSI C84.1 ranges (1.05 p.u.–1.06 p.u.). Also, the activation of volt-watt when combined with volt-var will depend on the effectiveness of volt-var to regulate voltage prior to directly decreasing active power output to prevent voltage violations. Volt-watt control is recommended as a backstop to occasional high voltages outside ANSI ranges. Because high voltages often cannot be predicted in advance, system-wide activation of volt-watt control can be beneficial.

5.3 Methods for Estimating PV Energy Curtailment

5.3.1 AMI-Based Curtailment Estimation

The proposed methodology for estimating PV energy curtailment from smart meter or advanced metering infrastructure (AMI) voltage assumes maximum possible curtailment per the volt-watt curve based on the smart meter voltage during the time period of interest, as shown in Figure 5.2.

At voltage V_A , the maximum possible curtailed power caused by volt-watt is P_A . This assumes that the inverter could have been at maximum power whenever voltage was more than 1.06 p.u.

The proposed methodology is formulated as follows:

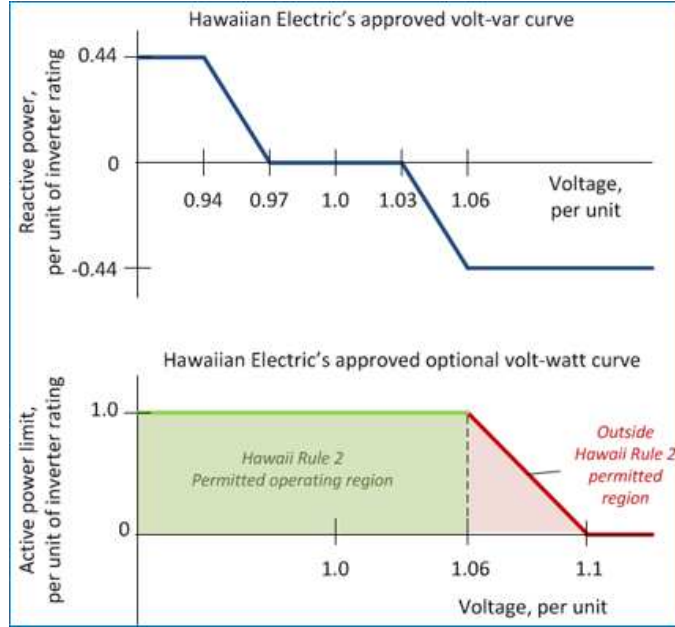


Figure 5.1: Hawaiian Electric's approved volt-var and proposed volt-watt curves

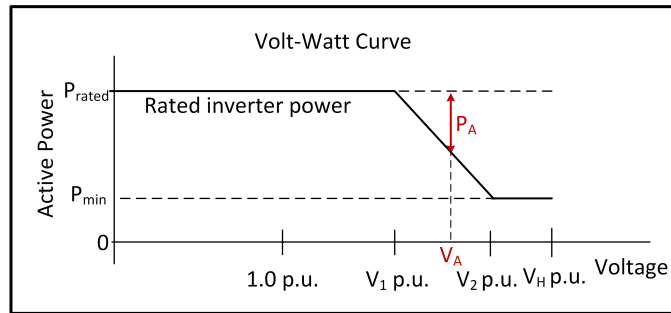


Figure 5.2: Volt-watt curve showing maximum possible curtailed power

$$E_{curt,i} = \sum_{V_{AMI,i}} \max\left(\frac{(V_{AMI} - V_1)}{V_2 - V_1}, 0\right) * (P_{PV,i} - P_{min,i}) * t_{AMI} \quad (5.1)$$

where E_{curt} is the maximum possible curtailment caused by volt-watt, in kWh for every PV customer 'i', during the time period of interest; P_{PV} is the rated AC power of the PV system, in kW; t_{AMI} is the period of the AMI measurements in hours (i.e., for 15-minute readings, t_{AMI} is 0.25); V_1 is the maximum voltage at which the system is permitted to produce its rated power; V_2 is the voltage at which the system is required to produce its minimum active power (P_{min}), and V_{AMI} represents the set of AMI voltage readings between 9 a.m. and 3 p.m., per unit. This time period

is chosen because it represents peak sun hours with a high tendency for high solar generation and lower residential demand, resulting in high voltages and possible PV production curtailment.

With reference to the Hawaiian Electric volt-watt curve in Figure 1, V_1 is 1.06 of the nominal voltage (V_N) and V_2 is 1.1 of V_N . For most inverters, the inveter's minimum active power (P_{min}) is zero. IEEE 1547 defines V_H as the voltage upper limit for DER continuous operation [25].

Figure 5.3 shows a conceptual illustration of the proposed methodology using Hawaiian Electric's volt-watt curve for a hypothetical day in which the voltage peaks at 1.1 p.u. (which is much higher than seen in field data and outside of tariff rules, but useful for illustrative purposes). As shown in Figure 5.3, when the voltage is at 1.06 p.u. or below, the estimated power curtailed, P_{curt} , is zero; at 1.08 p.u., P_{curt} is half the rated AC power of the PV system, while at 1.1 p.u., P_{curt} equals the rated AC power of the PV system. The energy curtailed is simply the integral of the power curtailed over time.

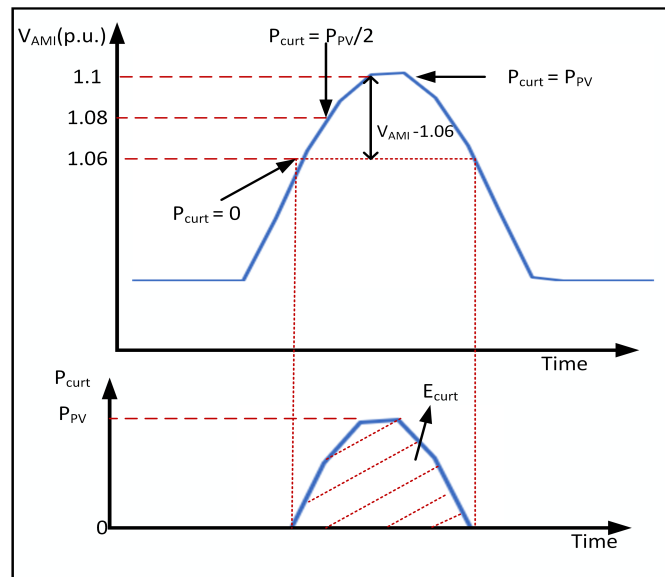


Figure 5.3: Conceptual illustration of estimated curtailment as a function of AMI voltage for a hypothetical day in which the voltage peaks at 1.1 p.u. (which is much higher than seen in field data and outside of tariff rules, but useful for illustrative purposes).

It is important to note that orientation and shading could impact PV system output and subsequent curtailment estimates, however because the curtailment estimation method presented here

is intended to provide a reasonable estimate without deployment of additional sensors or communications, characterizing the impact of shading on PV system output for the considered location topology, type of PV array (fixed or tracking) or the ground cover ratio, is beyond the scope of this study. Thus, the proposed methodology does not consider the impact of shading on PV system output.

Further, the behind-the-meter voltage analysis can be a complicated issue; in some cases behind-the-meter distributed generation is not even metered, which impacts the net imports or amount of generation needed for system balance [80]. Also, IEEE 1547-2018 now permits inverters to use the utility meter voltage for volt-watt control [25]. Thus, our proposed methodology did not consider the connecting wires between the inverter and the meter. In addition, this present study has been conducted based on the voltage set points or operating range as stipulated by the utility (shown in Figure 1), in this case Hawaiian Electric Rule 2 limits for character of service, which is based on the American National Standards Institute (ANSI) standard C84.1. For utilities with different voltage set points the results of our proposed methodology may vary, but the general principles described here are expected to hold.

5.3.2 Field Data-Based Curtailment Estimation

For field data curtailment estimates, a PV system with volt-watt activated, plane-of-array irradiance sensors, and local inverter power and voltage measurements are required. The procedure for the field measurements is as follows:

1. Obtain the actual measured inverter power (kW) values, P_{inv} .
2. Obtain irradiance-based estimates of maximum possible PV power (kW), P_{irrad} , based on a curve fit to the measured irradiance.
3. If $P_{inv} < P_{irrad}$, and inverter voltage (V_{dc}) $>$ threshold (where threshold = 430 VDC for this inverter configuration), and the measured inverter voltage is greater than 1.06 p.u., then the inverter is definitely in volt-watt mode.

4. To obtain the curtailed power, find the difference between P_{irrad} and P_{inv}

5.3.3 Simulation-Based Curtailment Estimation

In our previous study [35], we simulated a very high PV penetration scenario, with 10.9 MW of total PV installations for a network with 6.5-MVA peak load and 2.8-MVA minimum load. A high-voltage week was selected to capture PV production curtailed as a result of high voltage and the corresponding activation of volt-watt and volt-VAR control to mitigate the voltage limit violation.

The study includes primary and secondary (or low-voltage) circuits in the model, to explicitly represent individual customer connections and more accurately approximate the voltage at customer meter locations. The voltage simulated at the customer PCC is used as a simulation of meter or AMI customer voltage.

To estimate curtailment caused by voltage-based GSFs in the simulation-driven study, a baseline PV production scenario without the activation of volt-watt and volt-VAR control was first established and then compared with a PV deployment scenario with advanced inverter functions.

5.3.4 Metrics for Assessing Proposed Method Accuracy

To evaluate the accuracy of the proposed method, the following measures of accuracy are applied to the proposed AMI-based and VROS simulation-based results [?, 81–83]:

- Coefficient of determination (R^2 Score): This metric shows the proportion of variance in the observed data (in this case, the VROS simulation data) that can be explained by the proposed AMI-based curtailment estimation method. The best possible score is unity.

$$R^2_{score} = 1 - \frac{\sum_{j=1}^n (x_j - \hat{x}_j)^2}{\sum_{j=1}^n (x_j - \bar{x}_j)^2} \quad (5.2)$$

- Root mean square error (RMSE): The RMSE is used to quantify the error of the observed variance, with small values showing the optimality of the proposed method. An optimal prediction has an RMSE value close to 0.0.

$$RMSE = \sqrt{\frac{\sum_{j=1}^n (x_j - \hat{x}_j)^2}{n}} \quad (5.3)$$

- Mean absolute error (MAE): This metric measures the mean magnitude of the errors in a set of predictions, without considering their direction. It is defined as follows:

$$MAE = \frac{\sum_{j=1}^n (x_j - \hat{x}_j)}{n} \quad (5.4)$$

The best MAE value is 0.0.

- Mean squared logarithmic error (MSLE) = This metric penalizes underestimates more than overestimates, and it is given as:

$$MSLE = \frac{\sum_{j=1}^n (\log_e(1 + x_j) - \log_e(1 + \hat{x}_j))^2}{n} \quad (5.5)$$

An optimal prediction has an MSLE value close to 0.0.

- Explained variance score (EVS): This score measures the amount to which the proposed method accounts for variation in the VROS data set.

$$EVS = 1 - \frac{Var(x - \hat{x})}{Var(x)} \quad (5.6)$$

An optimal prediction has an EVS value close to unity.

- Median absolute error (MedAE): This metric computes the median of all the absolute differences between the given VROS data and the proposed AMI-based methodology. The advantage of this metric is that it is robust to outliers because outliers have a very small effect on the median. It is given as:

$$MedAE = median(|x_1 - \hat{x}_1|, \dots, |x_n - \hat{x}_n|) \quad (5.7)$$

An optimal prediction has an MedAE value close to zero.

where \hat{x}_j is the proposed AMI-based data of the j -th sample, x_j represents the corresponding VROS simulation data, \bar{x}_j is the mean of the VROS data, and n is the number of the data points.

5.4 Evaluating Methods for Estimating Curtailment

This section presents curtailment estimation based on the proposed AMI-based, VROS simulation and field measurement methods.

5.4.1 Curtailment Estimation Based on AMI and Simulation Voltages

As shown in Figure 5.4, the proposed AMI-voltage-based method of estimating curtailment aligns reasonably well with the VROS simulation, especially for the most-curtailed customers. For most customers located in the feeder with system-wide volt-watt activation, the PV production curtailed is negligible, as shown by both methods in Figure 5.4 for the high-voltage week.

Note that the VROS simulation captures all curtailment, not only volt-watt but also volt-VAR inclusive. Also, the PV systems with volt-VAR and volt-watt modeled in the VROS simulation had an assumption of a DC/AC ratio of 1.2, which also increases the curtailment experienced by customers because there are more time periods of high real power production.

It is also necessary to point out that high voltages are not always caused by local overgeneration by PV customers; there are other factors, such as constrained capacity of distribution transformers and overloading of the secondary conductors.

Customers with nonzero curtailment values are those with high voltages outside the ANSI C84.1 ranges (i.e., >1.05 p.u.). Thus, with voltage persistently or frequently above 1.06 p.u., volt-watt control can result in non-negligible curtailment. This is illustrated by our proposed methodology as shown in Figure 5.5 and Figure 5.6. For every voltage point in Figure 5.5 above 1.06 p.u., there is a corresponding energy curtailed as shown in Figure 5.6.

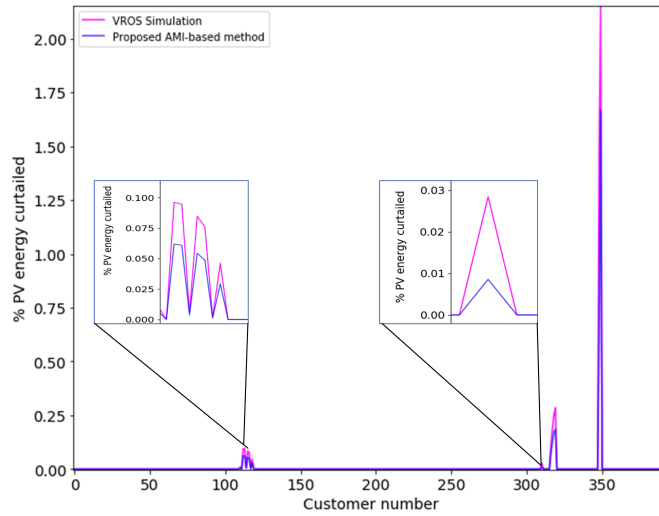


Figure 5.4: Proposed AMI-based method vs. VROS simulation curtailment estimates

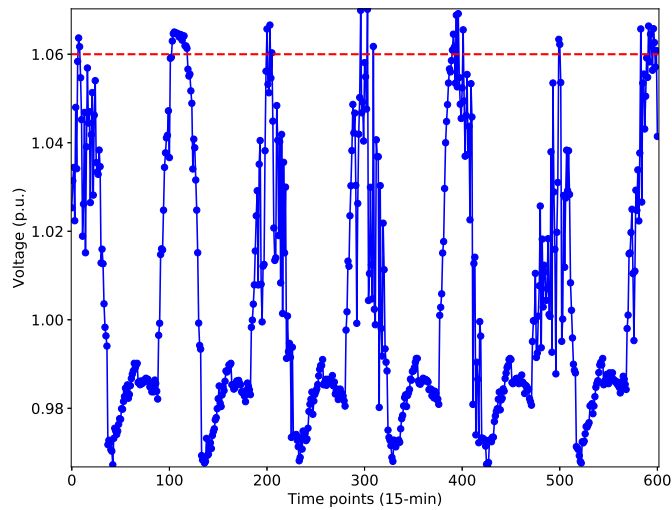


Figure 5.5: A typical high voltage customer from the VROS simulation

5.4.2 Curtailment Estimation Using Field Measurement

Two existing PV customers (locations A and B) with high-voltage issues were identified and instrumented to allow curtailment estimates. Many other field locations were evaluated but were not instrumented because voltages never or rarely exceeded 1.06 p.u. at most locations [84]. The measurement at one of the high-voltage locations from the advanced inverter location is shown in Figure 5.7.

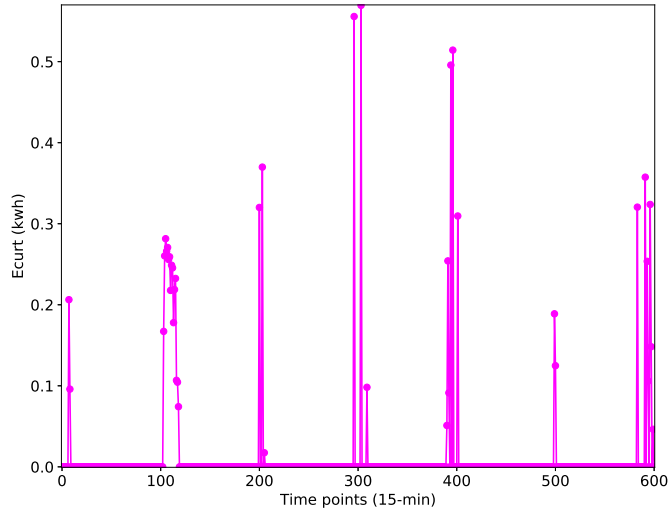


Figure 5.6: Curtailment estimates for the typical high voltage customer from the VROS simulation

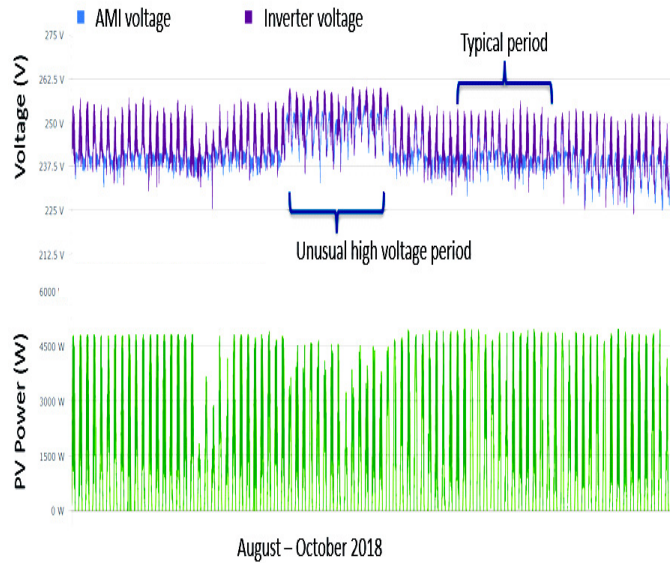


Figure 5.7: Field measurement at one of the selected advanced inverter locations

Two periods were selected for estimation of PV production curtailment: a normal typical condition without voltage violation and a high-voltage scenario. The high-voltage period as seen in Figure 5.7 occurred as a result of temporary feeder reconfigurations. The field data-based curtailment depends on the available solar resource, measured power, and behind-the-meter voltage.

Figure 5.8 shows the field measurement data for curtailment estimates during a high-voltage period for Location A. The dark blue dots connote the actual measured power as a function of solar irradiance, the red dots are estimated available power without curtailment as calculated from

measured irradiance (taking into account inverter characteristics), and the light blue dots represent actual measured inverter power at times when power was identified as curtailed based on irradiance measurements and inverter electrical data.

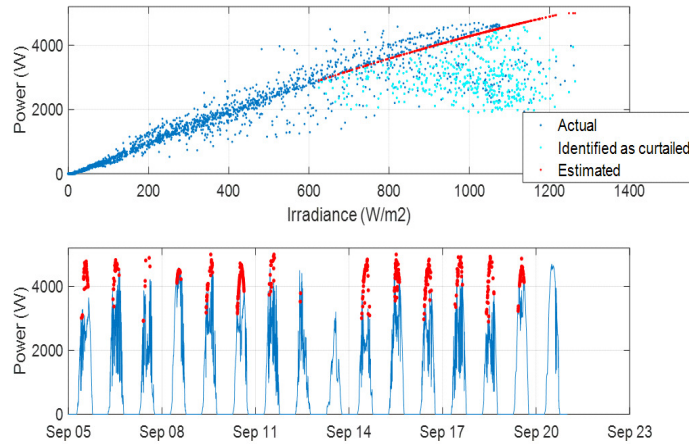


Figure 5.8: Field measurement-based curtailment estimates for a PV customer with volt-watt activation during a high-voltage period

Figure 5.9 shows a similar measurement and analysis during a normal voltage period for the same location. Figure 5.9 shows that the overall impact of volt-watt activation is greatly reduced during normal voltage conditions compared with the high-voltage period, as shown in Figure 5.8.

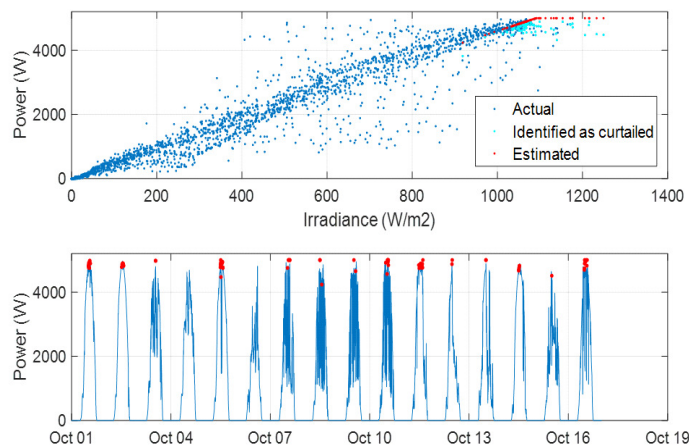


Figure 5.9: Field measurement-based curtailment estimates for a PV customer with volt-watt activation during a normal voltage period

PV inverters curtail power by moving their DC operating voltage away from the PV array maximum power point, i.e., moving away from the knee of the current-voltage curve. In some cases, it is possible for the DC-bus voltage to rise close to the PV array open-circuit voltage.

In Figure 5.10, the non-blue dots indicate elevated DC voltage, typically resulting from curtailment (for this inverter type, which uses DC:DC power optimizers on each PV module and thus has a predictable relationship between voltage and power when curtailed). This plot shows the non-negligible volt-watt curtailment during high-voltage periods (>1.05 p.u.).

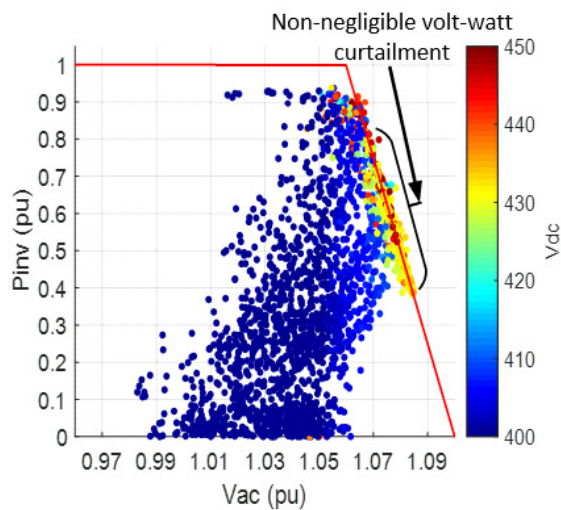


Figure 5.10: PV inverter power vs. AC voltage showing upper cutoff of the volt-watt curve and relationship to DC-bus voltage (dot color)

For the high-voltage period, the shape of the probability density function curve, shown in Figure 5.11, indicates that the voltage value of 1.05 p.u. has the largest probability. Also, at more than 1.05 p.u., there are voltage points with non-negligible probabilities.

5.5 Performance Evaluation

It is important to reiterate that the essence of this study is to compare our proposed methodology with our previous detailed VROS simulation and field data measurement at different periods. This section compares the result of the proposed AMI-based curtailment estimation method with the VROS simulation and field measurement data.

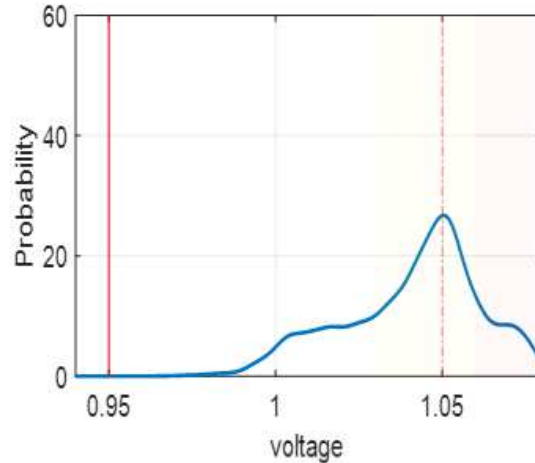


Figure 5.11: Probability density function for voltage data points during the high-voltage period

5.5.1 Comparing results of the proposed AMI-based curtailment estimation with the VROS simulation

To evaluate the accuracy of the proposed AMI-based curtailment estimation compared with the detailed VROS simulation, the metrics in Table 1 are considered. The optimal value represents the best possible value for each metric, whereas the computed value is the result of the comparison between the proposed method and the VROS simulation result.

The R^2 score shows that the proposed method captured 87% of the explained variance in the VROS data. This is further confirmed by the explained variance score of 87%. This indicates that 87% of the information in the VROS data is retained by the AMI-based method. Overall, the RMSE, MedAE, MSLE, and MAE values show that the proposed methodology aligns reasonably well with VROS simulation data.

5.5.2 Comparing results of the proposed AMI-based curtailment estimation with the field measurement data

For the purpose of comparing the proposed methodology with field measurement, two locations with high voltage issues were identified as described in subsection 4.0.2. Tables 2 and 3 show results for these specific locations over two different week periods. The VROS simulation has not

Table 5.1: Performance Metrics of the Proposed AMI-Based Methodology against the VROS simulation data

Metric	Optimal value	Computed value
Coefficient of determination (R^2 Score)	1.0	0.87
Mean absolute error (MAE)	0.0	0.004
Mean squared logarithmic error (MSLE)	0.0	0.0005
Explained variance score (EVS)	1.0	0.87
Median absolute error (MedAE)	0.0	0.0
Root mean square error (RMSE)	0.0	0.049

been included because one of the locations is not in the test feeder, and the other location was not added because of the difficulty in matching that customer in the field with the data in the test feeder.

Table 2 compares the field measurement- and proposed AMI-based curtailment estimation methods for Location A. During a typical period when the voltage is within the ANSI C84.1 range (0.95 p.u.–1.05 p.u.), the actual curtailment based on field measurement- and AMI-based methodology are 0.3% and 0%, respectively. The high-voltage period shows a slight (2.3%) over-estimation by the proposed method in Location A.

Table 5.2: Comparing Field- and AMI-Based Curtailment Estimation for a Customer in Location A

Time periods	Measured production (kWh)	AMI-based production est. (kWh)	Actual curt. (kWh)	AMI-based cur. est. (kWh)	Actual curt. (%)	AMI-based curt. est. (%)
Typical period	425.2	426.5	1.3	0	0.3	0
High-voltage period	385	431.7	46.7	62.1	12.1	14.4

Table 3 compares the field measurement- and proposed AMI-based curtailment estimation methods for Location B. During the typical period, the total energy curtailment estimates for both

methods are 0.01% and 0%, respectively, whereas the high-voltage period shows a slight (1.65%) overestimation by the proposed method in Location B.

Table 5.3: Comparing Field- and AMI-Based Curtailment Estimation for a Customer in Location B

Time periods	Measured production (kWh)	AMI-based production est. (kWh)	Actual curt. (kWh)	AMI-based curt. est. (kWh)	Actual curt. (%)	AMI-based curt. est. (%)
Typical period	197	197	0.01	0	0.01	0
High-voltage period	106.8	107.9	1.0	2.8	0.94	2.59

5.6 Conclusions

Volt-watt grid support function activation used to mitigate persistent high voltages caused by high-penetration PV systems depends on the voltage at the inverter terminals. This paper proposes an AMI-based methodology for estimating lost PV production caused by volt-watt activation. This method estimates maximum possible curtailment for a given volt-watt curve based on the customer smart meter voltage during the time period of interest. The proposed method provides a reasonably accurate estimate of curtailment using only smart meter voltage data. The result of the proposed method further confirms that the activation of volt-watt control has a minimal impact on PV energy curtailed.

Validation against detailed computer simulation for hundreds of customers and against field data with irradiance sensing and inverter data shows that the proposed methodology yielded satisfactory comparable results. The proposed methodology is very simple to implement because it is based on only AMI voltage data, without the need for additional sensors, communications infrastructure, or inverter data.

This methodology can be used by utilities, regulators, and solar developers to estimate the curtailment impacts to customers. In addition, the performance metrics used to evaluate the accuracy of the proposed method compared with the detailed VROS simulation show that the proposed

methodology aligns reasonably well with VROS simulation data. For instance, the coefficient of determination (R^2 score) shows that the proposed method captured 87% of the explained variance in the VROS data, which is further confirmed by the explained variance score of 87%. Also, RMSE, MedAE, MSLE, and MAE show that the proposed method yielded satisfactory results.

The proposed method could be used to estimate customer energy curtailment, which could inform future impact evaluation and compensation mechanisms for utilities leveraging customer-sited resources to mitigate high-voltage and defer or avoid future infrastructure upgrades.

Chapter 6

Conclusions and Potential for Future Work

This dissertation proposes modeling techniques and methods to study the impacts to the utility and to the customers of using DERs such as advanced inverters to provide voltage support. The work is novel in that it raises the importance of modeling low voltage secondary circuits, to more accurately represent the local voltage at each individual DER location to which autonomous advanced inverter functions respond to, as well as to study the effectiveness of real and reactive power injection along primary and secondary distribution networks.

The main conclusions of the research presented in this dissertation are outlined below

- Creating and validating baseline models of the current utility operations is important to compare with future scenarios in which customer sited resources are integrated in the planning and operation of distribution systems
- Generalizing a voltage rise across all secondary circuits is not a very accurate way of approximating the impact of secondary low voltage rise, even within the same construction type of overhead or underground designs.
- Primary voltages are relatively flat, and the bulk of the voltage rise due to increased DER penetration occurs in the service transformer and secondary circuits
- The bulk of the voltage support from advanced inverters absorbing reactive power in constant power factor or volt-var modes is effective at reducing the voltage rise caused by DERs across the distribution service transformer, and not effective at mitigating the voltage rise across the secondary conductors. This is due to reactive power being effective at lowering the voltage where there is a higher reactance component, i.e. at the transformer, versus the highly resistive components of the secondary conductors.

- The activation of voltage-based GSFs, such as volt-var and volt-watt, results in a positive average net generation change, since there is less energy curtailed due to the activation of the GSFs than there is generation prevented from tripping above 1.1 p.u. per IEEE 1547 [46].
- A new curve is proposed for plotting the customer energy curtailment versus customer maximum voltage, which shows that when customer peak voltages are maintained close to the ANSI C84.1 recommendations, customer energy curtailment from GSFs such as volt-var and volt-watt will be negligible or very low.

The research described in this dissertation has informed important policy and grid code changes in Hawai'i and California with the approved changes to Rule 14H and California Rule 21 DER Interconnection Standards requiring the activation of voltage advanced inverter grid support functions such as volt-var and volt-watt.

This work can be expanded in many directions for future work. In this thesis, the impact of using one same advanced inverter setting for all DERs, which is currently seen as a practical way for installers to comply with the new requirements to provide voltage support. However, in the future, utilities could consider to optimize the settings for individual DERs to provide more or less voltage support as needed, but the value of the added complexity is unclear. Taking it one-step further, the advanced inverter settings could also be optimized on a more operational basis throughout the day via a DERMS or ADMS type utility management system. The impact of optimal advanced inverter settings and set-points in voltage management and to customers is yet to be explored. Another area of future research is including other technologies such as battery storage. Battery storage, as with PV systems, has also come down in cost and is now being installed in residential homes. The impact of such technology collocated with PV systems in providing voltage support can be further explored, as well, as the impact on resiliency due to the added capability of sustaining power outages for residential customers. Finally, another topic that can be explored is including load control for voltage support. Home Energy Management Systems (HEMS) are a growing area of research that can be explored, to understand how potentially advanced inverters could be integrated into the planning and optimization routines of HEMS. The economic implications and business models for

leveraging customer-sited into planning and operation of the distribution grid is a research area that can be further expanded. The research presented in this dissertation shows that with the proposed advanced inverter settings in Hawai'i, which are very similar that the ones used in California and recommended in IEEE 1547-2018, the impact to customer energy production is minimal as long as voltages are maintained within ANSI C84.1 limits. However, there could be outlier customers, or utilities could chose to implement more aggressive advanced inverter settings, and the right level of compensation for such customers is yet to be evaluated. Finally, the issue of accurate representation of low voltage circuits is a topic that can be further expanded. Using directed graph theory to statistically identify typical secondary circuits from field collected data is a topic currently being explored after the work here presented. Another area of active research currently being explored by industry and other research organizations is to use an open maps API as well as heuristic rules from the statistical analysis of secondary low voltage circuits to trace secondary circuits for specific service transformer locations. This is currently being researched, after the work described in this thesis, in order to allow utilities to more accurately predict the impact of a DER, as well as to explore more innovating solutions to mitigate the adverse impact of a DER. Typically utilities propose a grid infrastructure upgrade when a DER is going to violate a voltage or a thermal constraint. However, with a detailed model of the distribution low voltage circuit, utilities could play with more innovative solutions such as battery storage, legacy inverter upgrades, optimal advanced inverter settings, etc. to mitigate the impact of a DER interconnection.

Bibliography

- [1] R. Rodriguez Labastida and D. Gauntlett. Market data: Global distributed solar pv business models, regulations, installed capacity, system prices, and revenue for distributed and non-distributed solar pv. pages 1–1, January 2017.
- [2] International Renewable Energy Agency. Electricity storage and renewables: Costs and markets to 2030. January 2017.
- [3] Southern California Edison. The emerging clean energy economy: Customer-driven, modernized, reliable. January 2017.
- [4] "ANSI C84.1" Voltage Ratings for Electric Power Systems and Equipment (60Hz). American National Standards Association, 1977.
- [5] JOINT CA IOU WHITE PAPER SERIES . Enabling smart inverters for distribution grid services. October 2018.
- [6] Sunspec Alliance. Common smart inverter profile.
- [7] Ieee standard for smart energy profile application protocol. *IEEE Std 2030.5-2018 (Revision of IEEE Std 2030.5-2013)*, pages 1–361, Dec 2018.
- [8] A. Nelson et. Al. Hawaiian electric advanced inverter grid support function laboratory validation and analysis. (NREL/TP-5D00-67485), December 2016.
- [9] M. Tahir, M. E. Nassar, R. El-Shatshat, and M. M. A. Salama. A review of volt/var control techniques in passive and active power distribution networks. In *2016 IEEE Smart Energy Grid Engineering (SEGE)*, pages 57–63, Aug 2016.
- [10] Ieee approved draft guide to conducting distribution impact studies for distributed resource interconnection. *IEEE P1547.7/D11, June 2013*, pages 1–129, Feb 2014.

- [11] B. A. Mather. Quasi-static time-series test feeder for pv integration analysis on distribution systems. In *2012 IEEE Power and Energy Society General Meeting*, pages 1–8, July 2012.
- [12] M. Baggu, R. Ayyanar, and D. Narang. Feeder model validation and simulation for high-penetration photovoltaic deployment in the arizona public service system. In *2014 IEEE 40th Photovoltaic Specialist Conference (PVSC)*, pages 2088–2093, June 2014.
- [13] M. Baggu, J. Giraldez, T. Harris, N. Brunhart-Lupo, L. Lisell, and D. Narang. Interconnection assessment methodology and cost benefit analysis for high-penetration pv deployment in the arizona public service system. In *2015 IEEE 42nd Photovoltaic Specialist Conference (PVSC)*, pages 1–6, June 2015.
- [14] Jeff Smith, Matthew Rylander, Jens Boemer, Robert Broderick, Matthew Reno, and B Mather. Analysis to inform ca grid integration rules for pv: Final report on inverter settings for transmission and distribution system performance. September 2016.
- [15] T. Boehme, A. R. Wallace, and G. P. Harrison. Applying time series to power flow analysis in networks with high wind penetration. *IEEE Transactions on Power Systems*, 22(3):951–957, Aug 2007.
- [16] Mohamed A. AbdelWarth, Mamdouh Abdel-Akher, and Mohamed Aly. Quasi-static time-series simulation of congested power systems with wind power plant. 12 2015.
- [17] J. R. AgÃijero, P. Chongfuangprinya, S. Shao, L. Xu, F. Jahanbakhsh, and H. L. Willis. Integration of plug-in electric vehicles and distributed energy resources on power distribution systems. In *2012 IEEE International Electric Vehicle Conference*, pages 1–7, March 2012.
- [18] S. Shao, F. Jahanbakhsh, J. R. AgÃijero, and L. Xu. Integration of pevs and pv-dg in power distribution systems using distributed energy storage â dynamic analyses. In *2013 IEEE PES Innovative Smart Grid Technologies Conference (ISGT)*, pages 1–6, Feb 2013.

- [19] T. Harris, A. Nagarajan, M. Baggu, and T. Bialek. Cost benefit and alternatives analysis of distribution systems with energy storage systems. In *2017 IEEE 44th Photovoltaic Specialist Conference (PVSC)*, pages 2991–2995, June 2017.
- [20] A. Nagarajan and R. Ayyanar. Design and strategy for the deployment of energy storage systems in a distribution feeder with penetration of renewable resources. *IEEE Transactions on Sustainable Energy*, 6(3):1085–1092, July 2015.
- [21] M. Kleinberg, J. Harrison, and N. Mirhosseini. Using energy storage to mitigate pv impacts on distribution feeders. In *ISGT 2014*, pages 1–5, Feb 2014.
- [22] D. Cheng, B. A. Mather, R. Seguin, J. Hambrick, and R. P. Broadwater. Photovoltaic (pv) impact assessment for very high penetration levels. *IEEE Journal of Photovoltaics*, 6(1):295–300, Jan 2016.
- [23] M. Reno A. Ellis J. Smith R.. Broderick, J. Quiroz and R. Dugan. Time series power flow analysis for distribution connected pv generation. January 2013.
- [24] M. J. Reno, J. Deboever, and B. Mather. Motivation and requirements for quasi-static time series (qsts) for distribution system analysis. In *2017 IEEE Power Energy Society General Meeting*, pages 1–5, July 2017.
- [25] Ieee standard for interconnection and interoperability of distributed energy resources with associated electric power systems interfaces. *IEEE Std 1547-2018 (Revision of IEEE Std 1547-2003)*, pages 1–138, April 2018.
- [26] Shriram S. Rangarajan, E Randolph Collins, J Curtiss Fox, and D.P. Kothari. A survey on global pv interconnection standards. pages 1–8, 02 2017.
- [27] Umid Mamadaminov. Advanced inverters and their functionalities for distributed solar generation. 07 2014.

- [28] A. Hoke, J. Giraldez, B. Palmintier, E. Ifuku, M. Asano, R. Ueda, and M. Symko-Davies. Setting the smart solar standard: Collaborations between hawaiian electric and the national renewable energy laboratory. *IEEE Power and Energy Magazine*, 16(6):18–29, Nov 2018.
- [29] F. Ding, A. Pratt, T. Bialek, F. Bell, M. McCarty, K. Atef, A. Nagarajan, and P. Gotseff. Voltage support study of smart pv inverters on a high-photovoltaic penetration utility distribution feeder. In *2016 IEEE 43rd Photovoltaic Specialists Conference (PVSC)*, pages 1375–1380, June 2016.
- [30] D. Ding et. Al. Photovoltaic impact assessment of smart inverter volt-var control on distribution system conservation voltage reduction and power quality. (NREL/TP-5D00- 67296), Dec 2016.
- [31] Z. K. Pecenak, J. Kleissl, and V. R. Disfani. Smart inverter impacts on california distribution feeders with increasing pv penetration: A case study. In *2017 IEEE Power Energy Society General Meeting*, pages 1–5, July 2017.
- [32] M. Bello, D. Montenegro, B. York, and J. Smith. Optimal settings for multiple groups of smart inverters on secondary systems using autonomous control. In *2017 IEEE Rural Electric Power Conference (REPC)*, pages 89–94, April 2017.
- [33] J. Seuss, M. J. Reno, M. Lave, R. J. Broderick, and S. Grijalva. Advanced inverter controls to dispatch distributed pv systems. In *2016 IEEE 43rd Photovoltaic Specialists Conference (PVSC)*, pages 1387–1392, June 2016.
- [34] J. Giraldez et. Al. Simulation of hawaiian electric companies feeder operations with advanced inverters and analysis of annual photovoltaic energy curtailment. (NREL/TP-5D00-68681), September 2017.
- [35] J. Giraldez et. Al. Advanced inverter voltage controls: Simulation and field pilot findings. (NREL/TP-5D00-72298), October 2018.

- [36] M. G. Kashani, M. Mobarrez, and S. Bhattacharya. Smart inverter volt-watt control design in high pv penetrated distribution systems. In *2017 IEEE Energy Conversion Congress and Exposition (ECCE)*, pages 4447–4452, Oct 2017.
- [37] J. Giraldez, P. Gotseff, A. Nagarajan, R. Ueda, J. Shindo, and S. Suryanarayanan. Distribution feeder modeling for time-series simulation of voltage management strategies. In *2018 IEEE/PES Transmission and Distribution Conference and Exposition (TD)*, pages 1–5, April 2018 ©IEEE. Reprinted, with permission, from Julieta Giraldez, Peter Gotseff, Adarsh Nagarajan, Reid Ueda, Jon Shindo and Siddharth Suryanarayanan, Distribution Feeder Modeling for Time-Series Simulation of Voltage Management Strategies, 2018 IEEE/PES Transmission and Distribution Conference and Exposition (TD), August 2018.
- [38] J. Peppanen, C. Rocha, J. A. Taylor, and R. C. Dugan. Secondary low-voltage circuit models: How good is good enough? *IEEE Transactions on Industry Applications*, 54(1):150–159, Jan 2018.
- [39] J. Peppanen, S. Grijalva, M. J. Reno, and R. J. Broderick. Distribution system low-voltage circuit topology estimation using smart metering data. In *2016 IEEE/PES Transmission and Distribution Conference and Exposition (TD)*, pages 1–5, May 2016.
- [40] J. Peppanen, S. Grijalva, M. J. Reno, and R. J. Broderick. Secondary circuit model generation using limited pv measurements and parameter estimation. In *2016 IEEE Power and Energy Society General Meeting (PESGM)*, pages 1–5, July 2016.
- [41] J. Peppanen, S. Grijalva, M. J. Reno, and R. J. Broderick. Secondary circuit model creation and validation with ami and transformer measurements. In *2016 North American Power Symposium (NAPS)*, pages 1–6, Sep. 2016.
- [42] J. Peppanen, M. J. Reno, R. J. Broderick, and S. Grijalva. Distribution system model calibration with big data from ami and pv inverters. *IEEE Transactions on Smart Grid*, 7(5):2497–2506, Sep. 2016.

- [43] V. Rigoni, L. F. Ochoa, G. Chicco, A. Navarro-Espinosa, and T. Gozel. Representative residential lv feeders: A case study for the north west of england. In *2016 IEEE Power and Energy Society General Meeting (PESGM)*, pages 1–1, July 2016.
- [44] M. Hernandez, T. J. Peppanen, Hubert, J. Deboever, M. McCarty, F. Petrenko, and O. Trinko. Test smart inverter enhanced capabilities— photovoltaics (pv): Smart inverter modeling report. (EPIC 2.03A), February 2019.
- [45] J. Giraldez, P. Gotseff, A. Nagarajan, R. Ueda, J. Shindo, and S. Suryanarayanan. Impacts of voltage-based grid support functions on energy production of pv customers. 2019 ©IEEE. Reprinted, with permission, from Julieta Giraldez, Michael Emmanuel, Andy Hoke and Sidharth Suryanarayanan, Impacts of Voltage-based Grid Support Functions on Energy Production of PV Customers, 2019 IEEE Power Energy Society General Meeting (PESGM), August 2019.
- [46] Ieee standard for interconnecting distributed resources with electric power systems. *IEEE Std 1547-2003*, pages 1–28, July 2003.
- [47] Ieee standard for interconnecting distributed resources with electric power systems - amendment 1. *IEEE Std 1547a-2014 (Amendment to IEEE Std 1547-2003)*, pages 1–16, May 2014.
- [48] B York. Arizona public service solar partner program advanced inverter demonstration results. *Electric Power Research Institute (EPRI)*, September 2017.
- [49] M. Rylander, J. Smith, and W. Sunderman. Streamlined method for determining distribution system hosting capacity. *IEEE Transactions on Industry Applications*, 52(1):105–111, Jan 2016.
- [50] J. Peppanen, M. Bello, and M. Rylander. Service entrance hosting capacity. In *2018 IEEE 7th World Conference on Photovoltaic Energy Conversion (WCPEC) (A Joint Conference of 45th IEEE PVSC, 28th PVSEC 34th EU PVSEC)*, pages 1451–1456, June 2018.

- [51] R. Carnieletto, S. Suryanarayanan, M. G. Simoes, and F. A. Farret. A multifunctional single-phase voltage source inverter in perspective of the smart grid initiative. In *2009 IEEE Industry Applications Society Annual Meeting*, pages 1–7, Oct 2009.
- [52] M. Rylander, M. J. Reno, J. E. Quiroz, F. Ding, H. Li, R. J. Broderick, B. Mather, and J. Smith. Methods to determine recommended feeder-wide advanced inverter settings for improving distribution system performance. In *2016 IEEE 43rd Photovoltaic Specialists Conference (PVSC)*, pages 1393–1398, June 2016.
- [53] S. R. Abate, T. E. McDermott, M. Rylander, and J. Smith. Smart inverter settings for improving distribution feeder performance. In *2015 IEEE Power Energy Society General Meeting*, pages 1–5, July 2015.
- [54] Peter Gotseff, Nick Wunder, Andy Hoke, Earle Ifuku, and Reid Ueda. Residential advanced photovoltaic inverter pilot study results for select distribution secondaries in hawaii. pages 1418–1423, 06 2018.
- [55] M. Emmanuel, J. Giraldez, P. Gotseff, and A. Hoke. Estimation of solar photovoltaic energy curtailment due to voltwatt control. *IET Renewable Power Generation*, 14(4):640–646, March 2020 ©The Institution of Engineering and Technology. Reprinted, with permission, from Michael Emmanuel, Julieta Giraldez, Peter Gotseff and Andy Hoke, Estimation of Solar Photovoltaic Energy Curtailment due to Volt-watt Control, *IET Renewable Power Generation*, March 2020.
- [56] M. Yazdani-Damavandi, N. Neyestani, G. Chicco, M. Shafie-khah, and J. P. S. Catalão. Aggregation of distributed energy resources under the concept of multienergy players in local energy systems. *IEEE Transactions on Sustainable Energy*, 8(4):1679–1693, Oct 2017.
- [57] S. Hu, Y. Xiang, J. Liu, C. Gu, X. Zhang, Y. Tian, Z. Liu, and J. Xiong. Agent-based coordinated operation strategy for active distribution network with distributed energy resources. *IEEE Transactions on Industry Applications*, 55(4):3310–3320, July 2019.

- [58] M. Choobineh and S. Mohagheghi. Robust optimal energy pricing and dispatch for a multi-microgrid industrial park operating based on just-in-time strategy. *IEEE Transactions on Industry Applications*, 55(4):3321–3330, July 2019.
- [59] Josue Campos do Prado, Wei Qiao, Liyan Qu, and Julio Romero Agüijero. The Next-Generation Retail Electricity Market in the Context of Distributed Energy Resources: Vision and Integrating Framework. *Energies*, 12(3):1–24, February 2019.
- [60] J. Deboever, J. Peppanen, N. Maitra, G. Damato, J. Taylor, and J. Patel. Energy storage as a non-wires alternative for deferring distribution capacity investments. In *2018 IEEE/PES Transmission and Distribution Conference and Exposition (TD)*, pages 1–5, April 2018.
- [61] J. H. Braslavsky, L. D. Collins, and J. K. Ward. Voltage stability in a grid-connected inverter with automatic volt-watt and volt-var functions. *IEEE Transactions on Smart Grid*, 10(1):84–94, Jan 2019.
- [62] G. Brinkman P. Denholm, M. O’Connell and J. Jorgenson. Overgeneration from solar energy in california: A field guide to the duck chart. Nov 2015.
- [63] J. P. Chaves-Avila, F. Banez-Chicharro, and A. Ramos. Impact of support schemes and market rules on renewable electricity generation and system operation: the spanish case. *IET Renewable Power Generation*, 11(3):238–244, 2017.
- [64] A. F. Hoke, M. Shirazi, S. Chakraborty, E. Muljadi, and D. Maksimovic. Rapid active power control of photovoltaic systems for grid frequency support. *IEEE Journal of Emerging and Selected Topics in Power Electronics*, 5(3):1154–1163, Sep. 2017.
- [65] T. Hiyama and K. Kitabayashi. Neural network based estimation of maximum power generation from pv module using environmental information. *IEEE Transactions on Energy Conversion*, 12(3):241–247, 1997.

- [66] M. Taherbaneh and K. Faez. Maximum power point estimation for photovoltaic systems using neural networks. In *2007 IEEE International Conference on Control and Automation*, pages 1614–1619, 2007.
- [67] Jen-Cheng Wang, Yu-Li Su, Jyh-Cherng Shieh, and Joe-Air Jiang. High-accuracy maximum power point estimation for photovoltaic arrays. *Solar Energy Materials and Solar Cells*, 95(3):843 – 851, 2011.
- [68] Gaurav Kumar and Ashish K. Panchal. Geometrical prediction of maximum power point for photovoltaics. *Applied Energy*, 119:237 – 245, 2014.
- [69] J. Seuss, M. J. Reno, M. Lave, R. J. Broderick, and S. Grijalva. Advanced inverter controls to dispatch distributed pv systems. In *2016 IEEE 43rd Photovoltaic Specialists Conference (PVSC)*, pages 1387–1392, June 2016.
- [70] Aadil Latif, Wolfgang Gawlik, and Peter Palensky. Quantification and mitigation of unfairness in active power curtailment of rooftop photovoltaic systems using sensitivity based coordinated control. *Energies*, 9(6):436, Jun 2016.
- [71] M. A. Shuvra and B. Chowdhury. Distributed dynamic grid support using smart pv inverters during unbalanced grid faults. *IET Renewable Power Generation*, 13(4):598–608, 2019.
- [72] A. B. Nassif, T. Greenwood-Madsen, S. P. Azad, and D. F. Teshome. Feeder voltage management through smart inverter advanced functions and battery energy storage system. In *2018 IEEE Power Energy Society General Meeting (PESGM)*, pages 1–5, Aug 2018.
- [73] S. Hempel, J. Schmidt, P. Gambn, and E. TrÄuster. Smart network control with coordinated pv infeed. *IET Renewable Power Generation*, 13(5):661–667, 2019.
- [74] K. Turitsyn, P. Sulc, S. Backhaus, and M. Chertkov. Local control of reactive power by distributed photovoltaic generators. In *2010 First IEEE International Conference on Smart Grid Communications*, pages 79–84, 2010.

- [75] M. G. Kashani, Y. Cho, and S. Bhattacharya. Design consideration of volt-var controllers in distribution systems with multiple pv inverters. In *2016 IEEE Energy Conversion Congress and Exposition (ECCE)*, pages 1–7, 2016.
- [76] M. Ghapandar Kashani, S. Bhattacharya, J. Matamoros, D. Kaiser, and M. Cespedes. Autonomous inverter voltage regulation in a low voltage distribution network. *IEEE Transactions on Smart Grid*, 9(6):6909–6917, 2018.
- [77] S. R. Abate, T. E. McDermott, M. Rylander, and J. Smith. Smart inverter settings for improving distribution feeder performance. In *2015 IEEE Power Energy Society General Meeting*, pages 1–5, 2015.
- [78] V. T. Dao, H. Ishii, and Y. Hayashi. Optimal smart functions of large-scale pv inverters in distribution systems. In *2017 IEEE Innovative Smart Grid Technologies - Asia (ISGT-Asia)*, pages 1–7, 2017.
- [79] A. Verma, P. P. Verma, A. V. Eluvathiangal, and K. S. Swarup. An intelligent methodology to improve distribution system operational parameters utilising smart inverter functionalities of pv sources. *The Journal of Engineering*, 2019(18):4799–4803, 2019.
- [80] North American Electric Reliability Corporation (NERC). Distributed energy resources: Connection modeling and reliability considerations. 2017.
- [81] Luis A. Diaz-Robles, Juan C. Ortega, Joshua S. Fu, Gregory D. Reed, Judith C. Chow, John G. Watson, and Juan A. Moncada-Herrera. A hybrid arima and artificial neural networks model to forecast particulate matter in urban areas: The case of temuco, chile. *Atmospheric Environment*, 42(35):8331 – 8340, 2008.
- [82] J. C. Gutierrez-Estrada, R. Vasconcelos, and M. J. Costa. Estimating fish community diversity from environmental features in the tagus estuary (portugal): Multiple linear regression and artificial neural network approaches. *Journal of Applied Ichthyology*, 24(2):150–162, 2008.

- [83] Inmaculada Pulido-Calvo and Maria Manuela Portela. Application of neural approaches to one-step daily flow forecasting in portuguese watersheds. *Journal of Hydrology*, 332(1):1 – 15, 2007.
- [84] S.A. DeLurgio. *Forecasting Principles and Applications*. Bibliyografya ve İndeks. Irwin/McGraw-Hill, 1998.

Appendix A

This section contains the copyrights of the published papers used in this dissertation.

©2018 IEEE. Reprinted, with permission, from Julieta Giraldez, Peter Gotseff, Adarsh Nagarajan, Reid Ueda, Jon Shindo and Siddharth Suryanarayanan, Distribution Feeder Modeling for Time-Series Simulation of Voltage Management Strategies, 2018 IEEE/PES Transmission and Distribution Conference and Exposition (T&D), August 2018.

©2019 IEEE. Reprinted, with permission, from Julieta Giraldez, Michael Emmanuel, Andy Hoke and Siddharth Suryanarayanan, Impacts of Voltage-based Grid Support Functions on Energy Production of PV Customers, 2019 IEEE Power & Energy Society General Meeting (PESGM), August 2019.

©2020 The Institution of Engineering and Technology. Reprinted, with permission, from Michael Emmanuel, Julieta Giraldez, Peter Gotseff and Andy Hoke, Estimation of Solar Photovoltaic Energy Curtailment due to Volt-watt Control, IET Renewable Power Generation, March 2020.